Northwestern | McCORMICK SCHOOL OF ENGINEERING

METALS: Metallic Expandable Technology for Artemis Lunar Structures

Final Report for NASA's 2024 Big Idea Challenge

Northwestern University

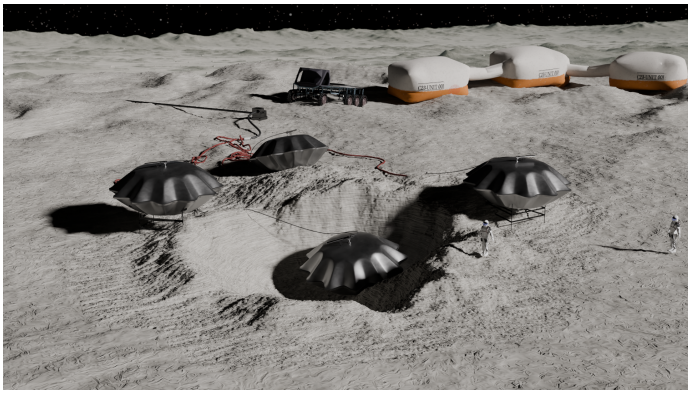

Team Leads: Trevor Abbott[2b*‡], Julian Rocher[12b*‡], Benjamin Taalman[12a*‡].

Team Members: Gavin Chung[2b*†], Victoria Israel[2be+†], Serena Frolli[2b+§], Charlize Guillen[2b*§], Sebastian Buckley Merce[2b*§], Enrique Montemayor[2c+§], Michael Bayer[2b*], Ty Bennett[2b*], Devan Chanda[2c*], Bobby Cloninger[2c*], Luke Fahrney[2d*], Omar Kamil[2c*], Joshua Natelson[2b*], Rahat Patel[2b*], Mingyuan Wang[2fg*], Liam Warlick[2a*], Tareq Mufarech[2a+], Spencer Guy[2b*], Xitlalli Castaneda[2b*], Jose Andres Vergara[2b+].

Faculty Advisor: Prof. Ian McCue[a] **Signature:** 10/16/24

Co-advisor: Prof. Ryan Truby[ab] **Signature:** 10/16/24

Space Grant Affiliation: Illinois Space Grant Consortium.

Space Grant Director Contact Information: Dr. Joshua Rovey, rovey@illinois.edu, (217) 300-7092

Industry Partners: National Aerospace Corporation, IMS Engineered Products.

NUSTARS Sponsors: Boeing Co; Epsilon3 Inc.; Onshape Inc.; The Murphy Society; Robert R. McCormick School of Engineering and Applied Science at Northwestern.

Northwestern University Space Technology and Rocketry Society (NUSTARS)
McCormick School of Engineering and Applied Science
October 16, 2024

1: MS Candidate. 2: Undergraduate. a: Department of Materials Science and Engineering. b: Department of Mechanical Engineering. c: Department of Electrical and Computer Engineering. d: Department of Chemical and Biological Engineering. e: Department of Biomedical Engineering. f: Department of Computer Science. g: Integrated Science Program. *: US Citizen. +: International Student. ‡: Team Lead, †: Interim Team Lead, §: Lead Engineer.

Metallic Expandable Technology for Artemis Lunar Structures (METALS)
Northwestern University

Concept Synopsis:

METALS is an inflatable system for long term cryogenic fluid storage on the Moon. Stacked layers of sheet metal are welded along their aligned edges, stacked inside a rocket, and inflated once on the lunar surface.
The manufacturing process is scalable, reliable, and simple. Modules can be buried under thermally insulative regolith for maximum energy efficiency during storage of fluid. Most importantly, METALS boasts superior performance in the harsh lunar environment, including resistance against radiation, abrasion, micrometeorites, gas permeability, and temperature extremes.

Image depicting concept

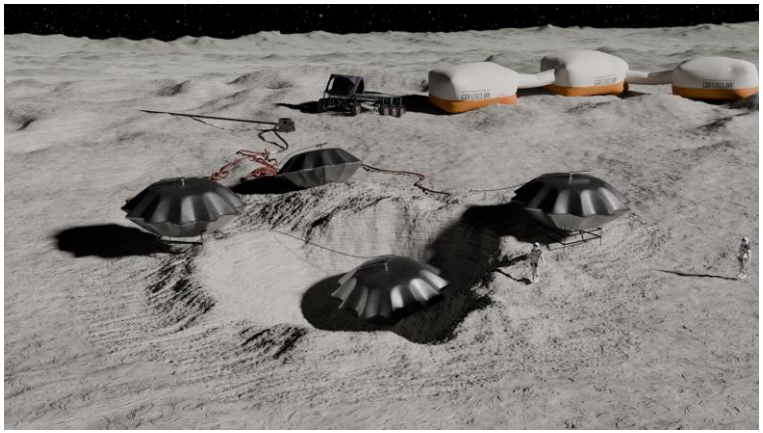

Innovations

- METALS manufacturing is proven to be scalable, consistent, and reliable.
- Developed an optimized inflatable geometry called the Sinusoidal Edge Curve (SEC) configuration which (1) reduces stress concentrations over the surface of the inflatable and (2) encourages controlled buckling, thus maximizing both the deployed volume of the inflatable and its maximum working pressure.
- Unlike other inflatable designs, the optimized SEC profile reached a consistent, self-similar deployed profile during inflation and retained that profile over a remarkable range of additional pressure without further deformation or failure, enabling safety, consistency, reliability for future lunar use.
- Inflation characteristics of SEC modules are shown to be consistent and favorably scale to higher volumes.

Verification Testing Results & Conclusions

- All SEC modules withstood high pressures and consistent inflation behavior, plateauing at a pressure dependent on the radius and thickness
- SEC modules provide adequate burst pressures and volumes for lunar deployment and use with cryogenic fluid
- METALS modules tested in a vacuum chamber perform with no irregularities in vacuum and with similar inflation characteristics as non-vacuum
- Metal modules will not fail when used for pressurized cryogenic storage, if inflated at higher temperatures and then filled with cryogenic fluid
- Punctures can be easily repaired using a metal patch or filler material
- Professional welds are free of any defects, while amateur welds do contain defects that are likely to impact performance
- Annealed modules demonstrate increased deformation

Table of Contents

1 Executive Summary

Inflatable technologies have long held promise as a key enabler for scaled lunar infrastructure development because of their capability to deploy into large structures from configurations which are densely-packed within the volume constraints of a lunar lander. However, the extreme environmental conditions of the lunar surface (including drastic temperature fluctuations, space irradiation, and abrasive lunar dust) make existing polymer-based inflatable designs largely unsuitable for long-term infrastructure development. This project, called **Metallic Expandable Technologies for Artemis Lunar Structures (METALS)**, utilizes the superior resistance of metal against lunar dust abrasion, micrometeorites, radiation degradation, gas permeability, and temperature extremes to provide unprecedented advancements in reliability and longevity compared to traditional polymer-based inflatables. Several applications of this technology are proposed, with particular emphasis on the use of METALS for scalable cryogenic storage on the lunar surface. This application is of especially significant value because no solution currently exists to effectively combine capabilities for cryogenic temperature storage with an inflation capability that permits scalable transportation within a lunar lander.

This project has demonstrated a rapid, affordable, and accessible method for manufacturing metal inflatables, in which two identical pieces of sheet metal are cut and welded at their aligned edges to create a small enclosed volume. After packing flat within a lunar lander, the inflatable can be pressurized and deployed to create large internal volumes. Critically, the metal deforms plastically during inflation, allowing it to maintain its deployed configuration even when internal pressurization is lost.

After the manufacturing method for the inflatable was developed, the team manufactured and tested over 300 different designs to study the behavior and performance of these inflatables. In parallel with parameterized finite element stress analysis, the team developed an optimized inflatable geometry called the Sinusoidal Edge Curve (SEC) configuration which (1) reduces stress concentrations over the surface of the inflatable and (2) encourages controlled buckling, thus maximizing both the deployed volume of the inflatable and its maximum working pressure. Unlike other inflatable designs, the optimized SEC profile reached a consistent, self-similar deployed profile during inflation and retained that profile over a remarkable range of additional pressure without further deformation or failure, enabling safety, consistency, reliability for future lunar use.

To verify METALS' advancement to TRL 5 maturity, the team first completed verification testing to confirm reliability and consistency in manufacturing methods and inflation behavior. This was followed by a variety of inflation testing campaigns to understand how the inflatable technology would perform within relevant lunar conditions, including inflation within a vacuum chamber and inflation/pressurization at cryogenic temperatures. The team also completed a variety of analyses which address various aspects of the planned mission scenarios for METALS, including development and verification of a method for repairing inflatables that have been damaged or punctured by micrometeorite debris. Furthermore, the team proposed burying the inflatables under an ~40 cm layer of regolith for exemplary radiation shielding, micrometeorite protection, and thermal insulation without any mass penalty of transporting additional material to the Moon. Via finite element thermal analysis, the insulativer performance of this regolith layer was determined to be sufficient for maintaining temperatures for cryogenic storage without excessive energy consumption.

This project has developed a solution for the cryogenic storage needs of a future Artemis lunar base camp by: (1) demonstrating a reliable, scalable, and exceptionally-simple manufacturing method for metal inflatable technologies, (2) optimizing a metal inflatable design for maximum deployed-to-stowed volume of fluid storage vessels, especially for cryogenics, and (3) evaluating the inflatable design within a variety of relevant lunar conditions, thus advancing metal inflatable technologies to TRL 5 status.

2 Problem Statement and Background

2.1 Introduction

The growth of a sustained human lunar presence will require infrastructure that can be efficiently packed within the volume constraints of lunar landers and deployed to far larger form factors on the lunar surface. Inflatable technologies are a promising solution to this need, but existing polymer-based inflatables are susceptible to many pervasive lunar conditions–including lunar dust abrasion, micrometeorites, radiation degradation, and temperature extremes–making them largely unsuitable for long-term lunar infrastructure development. Metal-based inflatables can provide extraordinary improvements against each of these environmental hazards (see Table 1), thus enabling the packing and deployability advantages of inflatable technologies with survivability characteristics suitable for the rapid and sustainable development of a permanent human lunar presence.

Table 1: Comparison of Polymer-Based Inflatables and METALS

	Traditional Polymer-Based Designs	Metal-Based Inflatables (METALS)
Environmental Hazards		
Micrometeorite and Orbital Debris	Loss of rigidity if punctured, extremely difficult to repair	Maintains deployed shape when punctured; easily repaired
Lunar Dust	Abrasion readily causes punctures, broken filaments, and loss of strength	High hardness ensures resistance to lunar dust abrasion
Temperature Extremes, Thermal Gradients from Sun-Side Heating	Unsuitable during lunar nights or within PSRs due to embrittlement at low temps	Maintain functional material properties across large temperature range; resistant to uneven heating due to ductility and high thermal conductivity
Radiation	Susceptible to degradation from intense solar and space radiation	Unlikely to be degraded by radiation over operational lifetime
Operational Characteristics		
Gas Conservation	Higher permeability constants K_p ($in^3/in^2/s$) than metals	Negligible gas permeation rates (excluding hydrogen)
Structural Rigidity	Rigidizing polymers concepts have fixed, unalterable shape; non-rigidizing concepts depend on constant internal pressurization	Plastically deformed to final configuration; does not require pressurization to retain shape after deployment
Reliability and Repairability	Difficult to repair/restore; poor longevity requires more frequent replacement; nearly impossible to repurpose	Higher ductility/toughness increases longevity and reduces need for replacement; can be melted down for reuse; easy to repair via welding
Manufacturing and Business Case	Requires advanced manufacturing materials, techniques, and machinery; complex/expensive supply chain	Simple, well-developed, and scalable manufacturing; affordable materials; simple, low-risk supply chain with diverse number of potential suppliers

2.2 Solution

The use of metal for inflatables enables the use of greatly simplified and readily-accessible manufacturing methods. The proposed technology, **Metallic Expandable Technology for Artemis Lunar Structures (METALS)**, is created by cutting and welding two identical pieces of sheet metal at their aligned edges to create a sealed volume. Once welded, these flat modules can be densely stacked within the payload volume of a lunar lander, similar to how shipments of stock sheet metal are stacked horizontally and transported on Earth. After reaching the lunar surface, each METALS module will be pressurized to plastically deform into its final configuration. This permanent deployment presents another key benefit of METALS over the current state of the art: while existing polymer-based inflatables require constant pressurization to maintain their shape, the plastic deformation of metal inflatables allows them to maintain their deployed configuration even if the gas inside is removed. Furthermore, the simplicity of METALS' manufacturing method stands in contrast to the complex, highly-specialized manufacturing of traditional polymer-based inflatables, thus enabling METALS to achieve accelerated production times, reduced fabrication costs, and accessible entrance by a plethora of commercial suppliers. These benefits streamline the further scaling, optimization, and flight qualification of metal inflatable technologies, **making METALS a near-term, high value solution relevant for Artemis missions within this decade.**

Additionally, METALS can be repaired just as easily as it is manufactured. Whereas torn or punctured polymer-based inflatables are extremely difficult to repair in a space environment, METALS can be

readily repaired in the lunar environment using standard welding techniques (see Section 4.2.5), further reducing the need for redundancy in launch manifests and cargo missions with replacement hardware.

Metal inflatable technology can be applied to a large variety of high-value lunar applications, including, but not limited to, high volume storage vessels, pipelines for transporting fluids, and structural members for infrastructure including lunar gantries, habitats, and towers. A use case where METALS shows exceptional promise for Artemis' goals is the storage of fluids–especially cryogenic fluids. A sustained human lunar presence will require extensive storage capacity of oxygen and other cryogenic fluids for both life support and the refueling of spacecraft–a need which becomes especially important within the context of NASA's Moon to Mars Architecture. However, there is **currently no viable solution for providing long-term lunar cryogenic storage in the capacities needed for refueling spacecraft on the Moon [1].** Traditional polymer-based inflatables lose their toughness at cryogenic temperatures, and no metal- or composite-based cryogenic solutions have been designed to be inflatable/deployable. Resultantly, the transport of fixed-shape, rigid tanks constitutes the current state-of-the-art in lunar cryogenic storage. This solution is inherently volume-prohibitive, as no spacecraft can transport a payload of rigid tanks with enough volume to meet the refueling requirements of that same spacecraft–even less the refueling requirements of a growing fleet of spacecraft during the rapid development of a sustained lunar presence. Metal inflatables thus provide the inevitable solution to the Artemis requirement for scalable lunar cryogenic storage: METALS combines a materials class suitable for mechanical loading (pressurization) under cryogenic temperatures, with an inflation capability that enables storage and transport within a lunar lander's payload volume.

2.3 Mission Scenario

The flat METALS modules will be densely stacked on one another within the payload volume of a lunar lander (visualize this as a package of stacked tortillas). After a module is offloaded from a lunar lander, it will be pressurized with gas and plastically deformed into its final deployed state. Before pressurizing, the inflatable can be placed in direct sunlight to elevate its temperature, giving the metal sufficient ductility and toughness to achieve the maximum possible localized strain–and thus the maximum achievable deployed storage volume (inflating with a preheated, inert gas can amplify this effect). This gas can be removed from the module post-inflation and used to deploy other units. The expanded inflatable can then be lowered into a hole dug by an autonomous lunar excavator (see NASA STMD's ISRU Pilot Excavator, or IPEx, program [2]), attached via piping to a cryogenic fluid distribution network, and finally buried under ~40 cm of regolith. The hardness of metal allows for direct contact with regolith (see Section 3.2.8), and the specific depth ensures periodic temperature fluctuations are dampened to less than a 10℃ range due to the highly insulative properties of regolith [3]. While burying under regolith is not required for the function of METALS, doing so provides effective protection from micrometeorites and radiation, while also enabling efficient thermal insulation for long-term cryogenic storage with minimal energy input (see Section 3.2.10). Most importantly, regolith is abundant on the Moon and can be continually accumulated above the inflatable until the desired level of radiation shielding, micrometeorite protection, and thermal insulation is achieved–all without contributing any additional mass to launch manifests.

Once the module is buried, it can be filled with fluid, most notably cryogenic fluid, produced via In-Situ Resource Utilization [4]. The cryogenic temperature will be maintained via a closed-loop system between the module and a cryocooler. Importantly, the cold temperatures of the cryogenic fluid will significantly increase the strength of the module's material (an austenitic stainless steel), restricting further yield at storage pressures. METALS therefore utilizes the drastic temperature differences on the Moon to advantageously operate the inflatable in two material regimes: the inflatable is heated in direct sunlight to enhance ductility and inflation, but then cooled with cryogenic fluid and insulated by lunar regolith to provide it with sufficient strength to maintain fluid storage pressures without bursting or further yield. By utilizing regolith protection and the Moon's extreme thermal environments, METALS is not just well equipped for the harsh lunar environment–it uses the lunar environment to its unique advantage.

3 Project Description

3.1 Technology Overview

Metallic inflatable technologies provide high-value deployment and functional capabilities to an Artemis lunar base while maintaining characteristics that are remarkably well-suited to the variety of harsh conditions of the lunar environment. However, metal-based inflatables remain underexplored and underdeveloped: no published information is available regarding the evaluation or qualification of such technologies for the lunar environment.

To advance lunar metallic inflatable technologies to TRL 5, this project addresses these needs by: (1) demonstrating a reliable, scalable, and simple manufacturing process, (2) optimizing a metal inflatable design for maximum storage of fluids, especially for cryogenics, and (3) evaluating the inflatable design within a variety of relevant lunar conditions.

The following project description primarily focuses on the identified use case for lunar cryogenic storage vessels, but much of the information presented (including manufacturing techniques, development methods, deployment scenarios, external/enabling lunar systems, and scalability considerations) is broadly applicable for any potential application of metallic inflatable technology, including fluid transport and piping, deployable towers, solar reflectors, structures, gantries and cranes, dust protection systems, and others.

3.2 Design and Optimization

The fundamental concept of METALS is to cut and weld two identical pieces of sheet metal at their aligned edges to create a sealed volume. Once welded, the interior is pressurized to plastically deform the sheet metal into its final deployed state, transforming a flat, two-dimensional design into a complex, three-dimensional structure. The design space for METALS is thus defined exclusively by the two-dimensional shape that is cut from stock sheets of metal, along with a selection of the alloy, sheet metal thickness, and inflation pressure of the inflatable. With a focus on the application of cryogenic storage, the performance criteria for the design is the volume of internal fluid storage that can be provided per mass of inflatable transported to the lunar surface, i.e., cubic meters of deployed internal volume per kilogram of sheet metal. (This performance criteria was not chosen on a per volume of metal basis because the flat, undeployed inflatables can be stacked so densely within a lunar lander that the capacity provided by a payload of inflatables will always be mass-limited, not volume limited. Furthermore, the performance criteria is based on the volume of internal storage provided rather than the mass of fluid storage provided because the density of cryogenic liquids is largely pressure-independent. As a result, any design which can withstand the minimum pressure requirements for liquid storage is both feasible and otherwise equivalent in performance. Optimization of the design therefore requires the selection of an alloy, sheet metal thickness, inflation pressure, and two-dimensional sheet metal shape that maximizes the internal volume per mass of sheet metal (under the constraint that the design can withstand the required pressures for fluid storage, see further details below). Each of these decision variables was investigated in order to determine an optimal design which is both feasible for cryogenic storage pressures and scalable to meet the volumetric storage requirements of a future Artemis lunar base camp (see Section 4, Verification Testing and Conclusions).

Table 2: Formulation of Design Optimization for METALS

Design Parameters	Inflation pressure (P_I) , sheet metal thickness (t), 2D geometry of sheet metal, and alloy selection
Constraints	$P_I <$ (Burst Pressure) ; $P_I \geq$ (Storage Pressure)
Key Performance Parameter (KPP)	Maximize: (Deployed Volume)/(Sheet Metal Mass)

3.2.1 Selection of Sheet Metal Alloy

Prototypes of an array of alloy selections were manufactured and tested, including aluminum alloys, carbon steel, and stainless steel. Initially, aluminum was a promising selection due to its high specific strength and ubiquitous use as an aerospace structural material. However, poor weldability of aluminum alloys necessitated the use of filler metal that resulted in stiff, brittle welds and inferior performance (Figure 1). In contrast, the superior weldability of carbon steel enabled high-quality, ductile welds without the use of filler metal. These welds permitted the carbon steel to withstand very high localized strains without bursting, resulting in high volumetric expansion. Similar benefits were observed in stainless steel, which became the alloy of choice for the final design due to its superior specific strength over carbon steel, corrosion resistance, and favorable mechanical properties at cryogenic temperatures..

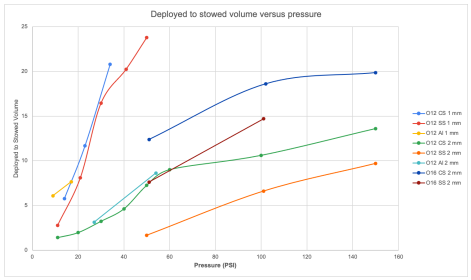

Figure 1: Deployed to stowed volumes for octagon inflatables for a variety of materials and thicknesses

3.2.2 Selection of Sheet Metal Thickness

Inflation testing of a variety of inflatable geometries and sheet metal thicknesses were completed (see Section 4.2.2 for details). In practice, the sheet metal thickness will be readily selected for a given fluid storage mission scenario such that the inflatable weight is minimized while processing sufficient strength to withstand target fluid storage pressures without bursting.

3.2.3 Selection of Inflation Pressure

Several test campaigns were completed to study the effect of inflation pressure on the resulting shape and internal volume of the inflatable (see Section 4.2.3 for details). Most inflatable designs continue to increase in volume with increasing pressure until the burst pressure is reached. However, the team's optimized inflatable design (see Section 3.2.4) deploys to a consistent, self-similar shape at a pressure far below its burst pressure; the inflatable then maintains its same shape without additional deformation for a remarkably large margin of additional pressurization before bursting. As a result, the optimal inflation pressure is simply equal to the pressure at which the inflatable's internal volume does not continue to increase. This selection maximizes the fluid storage capacity of the inflatable while eliminating the risk of bursting during deployment.

3.2.4 Selection of Two-Dimensional Sheet Metal Shape

The ideal shape for maximizing internal volume per area of sheet metal is a sphere. However, the manufacturing method for METALS requires the final three-dimensional deployed shape to originate from a two-dimensional one, and a hemisphere cannot be perfectly flattened into a plane. The optimization of the two-dimensional cut of the sheet metal is thus defined by the pursuit of a shape that transforms into a high-volume deployed shape with minimal distortion and stress; this optimization can be likened to the creation of projections that minimize the distortion of transforming a spherical globe into a two-dimensional map.

When inflating a two-dimensional sheet to a three-dimensional shape, experiments demonstrated that some amount of buckling and distortion in the inflatables is inevitable. Such instabilities are expected as no flat shape can perfectly accommodate a transformation into the third dimension. However, it was

discovered that certain shapes can be designed to “accommodate” this distortion by providing pathways for controlled, predictable buckling into a three-dimensional deployed state. Stated in more physical terms, a shape which would minimize the highest localized stress observed across the design during inflation while maximizing the resulting internal volume is desired. This optimization was completed using Ansys Mechanical software (see details in Section 3.2.5 FEM and Optimization below). Initial simulations demonstrated that incorporating a sinusoidal function to the outer radius significantly reduced stress concentrations and enhanced volumetric expansion. The optimized shape, referred to as the “Sinusoidal-Edged Circle” or “SEC”, is defined in polar coordinates by the following equation, where r represents the radial distance and θ is the angle:

$$r = R + A\cos(F \cdot \theta) \qquad 0 \leq \theta < 2\pi$$

This equation includes three parameters: base radius (R), amplitude (A), and frequency (F). While the base radius is often fixed to meet volumetric storage requirements, the amplitude and frequency can be adjusted to balance volume and stress.

Figure 2: Images of optimized Sinusoidal-Edged Circle (SEC) design before and after deployment.

3.2.5 Methods of Finite Element Stress Analysis for Design Prediction and Optimization

An optimal sheet metal shape is one that permits high-volume inflation without buckling instabilities and localized stress concentrations that would otherwise cause weld failures at unacceptably low pressures. The rapid and affordable manufacturing method created for METALS enabled rapid testing and iteration of many designs, but the use of finite element stress analysis via Ansys Mechanical enabled the fine-tuning of shape parameters and the rapid exploration of a much larger design space. Ansys ACT scripts automated the simulation workflow to enable the simulation of over 1000 design points (Figure 3). Both experiments and simulations determined that the ideal amplitude was approximately 5.5% of the radius. Furthermore, both approaches displayed that higher truncation factors (a parameter increasing the sharpness of an SEC peak) enabled increased volumetric expansion through the reduction of localized stress concentrations. The discrepancy between the optimal design in experiment and simulation arises from the inability to simulate convergence at truncation factors exceeding 4, but the presence of an optimal simulated point at the boundary of the investigated design space affirms the trends observed in experiment.

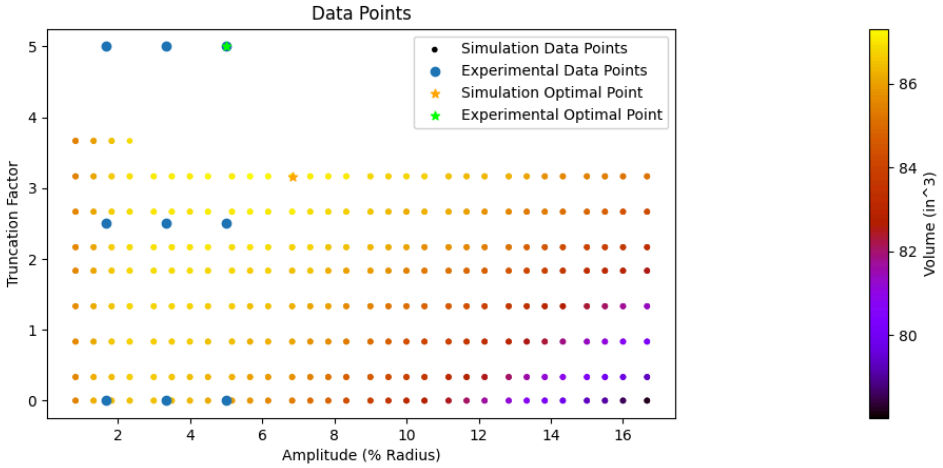

Figure 3: Geometry optimization data points from simulation and experiments.

3.2.6 Manufacturing Techniques

The optimized two-dimensional sheet metal shape can be cut from stock sheet metal using a Flow Mach 100 CNC waterjet. After all of the edges had been deburred in preparation for welding, a 3/8" hole was drilled into one of the two cut metal sheets using a drill press to accommodate a threaded pipe fitting for inflation. The fitting was first buttwelded with filler rod around the inflation hole. Then, that sheet was aligned on top of the second and the perimeter was edge-welded together. Tungsten Inert Gas (TIG) welding was selected due to its compatibility with thin metals, versatility across alloy types, and capacity for making precise, high-quality welds. A Miller Maxstar 280 DX TIGRunner running at 25-40 amps was utilized for all in-house prototype manufacturing. After completing these steps, the inflatable design was ready for testing.

Additionally, an industry partnership was formed with IMS Engineered Products (a global metal manufacturer in Des Plaines, IL), for the production of additional inflatable prototypes. The IMS team was provided with each design's drawing files, who then laser cut the design in the requested material and TIG welded the inflatable. Test modules were brought to Northwestern for inflation testing and analysis. The professional welders at IMS were able to produce reliable, quality welds for test articles up to 47 inches in diameter, allowing for assessment of how the experience and skill of the welder can affect the performance of the resulting inflatable. While welds created by IMS technicians were indeed of astounding quality, it is notable that team members were also able to hand-weld successful prototypes with little welding experience. This success can attest that welds of sufficient quality for inflation can be achieved with relative ease and high reliability, allowing for unexpectedly rapid production and iteration of prototypes. Furthermore, the success of hand-welding allowed the team to avoid the anticipated cost of a robotic welder and allocate those funds toward the purchase of additional material for testing.

In total, more than 300 inflatables were produced, including a variety of shapes (circle, pill, hexagon, SEC, TSEC), materials (Al 6061, stainless steel 304, stainless steel 321, and low-carbon steel 1008), and thicknesses (from 0.02" to 0.09"). Data and results of these tests are included in section 4.2.2 and 4.2.3.

3.2.7 Inflation Techniques

Once the prototypes were welded, inflation testing could commence. Inflation was accomplished using an air compressor and an air hose, which was threaded into a 1⁄4" NPT On/Off valve that controls the air flow. The valve screws into a tee connector that has two outputs: a pressure gauge and the output to the

inflatable. The output hose screws into the 1⁄4" NPT butt weld on the inflatable. A pressure washer was also used to inflate at greater pressure ranges.

3.2.8 Resistance to Abrasion

Fabrics such as Kevlar, Vectran, and Orthofabric are susceptible to abrasion due to the failure and fraying of individual fibers, conversely bulk metals are much more resilient to abrasion. Since metal surfaces are solid and continuous, they lack the interwoven fibers and crevices found in Kevlar, preventing regolith particles from embedding themselves and breaking down the material. Metals are also characterized by a higher material hardness index, enabling them to better withstand the sharp, abrasive particles in regolith without deforming or wearing away, making them far more durable in harsh lunar conditions and well-suited for direct contact with regolith (such as burying METALS modules).

3.2.9 Selection of Target Storage Temperature and Pressure

As described in Section 4.2.2, it is desirable to inflate the METALS units using the highest possible pressure that it can withstand (without bursting) to maximize the internal volume available for fluid storage. However, the pressure that the inflatable will need to withstand is also constrained by the minimum pressures required to maintain cryogenic fluids in liquid state. The cryogenic liquids that METALS would most likely target for long-term storage is methane (as a propellant for lunar landing craft) and oxygen (for usage as propellant and in life support). The below figure displays the liquid-vapor saturation curves for methane and oxygen, where the feasible region for liquid storage is defined above each curve. Cooler storage temperatures are desirable to reduce the stress on the inflatable and to increase the density of the resulting fluid. With target storage temperatures of 70 K for oxygen (above its triple point temperature of 55 K) and 95 K for methane (above its triple point temperature of 90.7 K), both oxygen-storing and methane-storing units should be expected to withstand pressures of at least 1 bar (regardless of scale) to provide at least 15 K of "thermal buffer" for the fluid to increase in temperature before the inflatable can no longer withstand the pressures required to maintain liquid storage. In the event that cooling capacity is lost for an extended period and excessive temperature increases in the fluid drive the required liquid storage pressure beyond the strength capacities of the inflatable, an emergency release valve would trigger to release fluid to the environment and prevent loss of the inflatable (see Section 3.3).

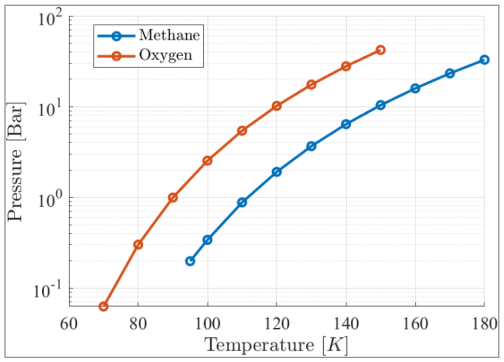

Figure 4: Graph of liquid-vapor saturation curves for methane and oxygen.

3.2.10 Validation of Regolith Thermal Performance

Burying inflatable units under a layer of regolith provides effective protection against radiation and micrometeorite damage. However, the most remarkable benefit provided by this layer of regolith is that of thermal insulation: the exceptionally low thermal conductivity of lunar regolith creates an effective barrier against the extreme temperature fluctuations of the lunar day/night while ensuring that any stored cryogenic fluid can be maintained at its target storage temperature with minimal energy consumption. To evaluate the insulative performance provided by the regolith and the resulting energy required to maintain liquid cryogenic storage in the proposed METALS system, a finite element thermal model was created. The model's two-dimensional axisymmetric geometry centers on an ellipsoidal shape representing a buried inflatable. (An ellipsoid with aspect ratio of 1:0.4–approximately equal to a deployed SEC design–was used as a simplified two-dimensional representation of the inflatable). Surrounding the outline of the inflatable is the regolith region where the thermal map is solved. Across the model's implementation, uncertainties were assessed with high conservatism, as summarized below:

- The highest thermal gradients (and thus rate of heat transfer) between the cryogenic liquid and regolith would occur when the regolith surface is heated by direct sunlight. While the lunar day/night cycle will reduce this average surface temperature, the thermal model was solved in under a steady-state solar heat flux of

$$S = S_0 \cdot a \cdot cos(\alpha) = 1421 \frac{W}{m^2} \cdot 1 \cdot cos(85^o) = 124 \frac{W}{m^2}$$

  calculated according to DSNE guidelines [5] for solar flux at a latitude of $\alpha = 85$ degrees (approximately equal to that of a planned Artemis base camp on the lunar south pole), where S_0 is the maximum solar constant and $a = 1$ is a conservative value for the solar absorptivity of regolith. By solving in steady-state, the model solves within an extremely conservative (hot) thermal environment of perpetual direct sunlight. This assumption has merit within the context of an Artemis basecamp near the rim of Shackleton Crater, where near-constant sunlight is expected.

- The emissivity of regolith was chosen as the lowest value given by DSNE (0.95) [5] while radiating to a deep-space temperature of 5 K.
- The only material property required is that of the thermal conductivity of regolith, adapted from DSNE as follows:

Regolith Depth (cm)	Thermal Conductivity (W/m-K)
0 to 2	0.0012
2 to 15	0.0125
35 to 234	0.02335

Table 3: Thermal Conductivity of Regolith with Respect to Depth [5]

- Finally, the entire surface of the inflatable was set to a fixed temperature of 70 K, representing the lowest storage temperature that would be reasonably targeted for liquid oxygen storage (the cryogenic fluid with the lowest temperature requirements). After solving for the resulting temperature field in the regolith, the total heat flow (in Watts) through the surface of the inflatable was calculated. This boundary condition assumes that the entire contents of the fluid and inflatable are maintained at or below 70 K, thus the resulting heat flow through the inflatable's exterior surface from the surrounding regolith constitutes the required thermal energy to maintain the target temperature in steady-state. Finally, the "far-field" temperature of the regolith at depths far beyond the inflatable was set to a fixed temperature of 132.5 K in accordance with averaged regolith temperatures at depths where thermal fluctuations caused by day-night cycles are not observed. The lack of thermal influence of the tank on the "far-field" boundaries is evidence that the selected domain is sufficiently large for these boundary conditions to be confidently applied as semi-infinite.

Notably, the boundary conditions selected above resulted in a regolith surface temperature of 219 K at distances far from the inflatable. DSNE stated that maximum surface temperatures within these lunar latitudes reach nearly the exact same temperature (224 K), providing validation that the selected boundary conditions result in an accurate model of lunar thermal conditions.

Images of the grid and an example solution are shown below, along with results for a variety of inflatable sizes (defined by major axis diameter with fixed aspect ratio of 0.4) and burying depths (defined by the distance from the top of the inflatable to the regolith surface. The energy expenditure required to cool the inflatable increases as the size (and therefore surface area) of the inflatable increases, or as the burying

depth decreases. However, the results also show that the energy expenditure required per volume of liquid stored decreases significantly as the inflatable size increases. While some of this effect is caused by the deeper average burying required for larger inflatables, it is also caused by the increased volume-to-surface area ratio with size. The conservatism of this analysis permits us to conclude that burying depths of at least 0.4 meters and inflatables of manufactured diameter of at least 4 meters can maintain cryogenic temperatures for no more than 2 W per cubic meter of liquid oxygen storage. This value is sufficient for storing the entire propellant capacity of Starship HLS (1052.6 m^3) [6] for just 2105 Watts. It is notable that increased pressure will lower temperature requirements and increase fluid density, yielding more efficient storage. This energy metric is easily scalable under anticipated lunar power availability (e.g. NASA's 40 kW Fission Surface Power Program [7]), even when accounting for mechanical and electrical losses in the temperature management system. Furthermore, the technologies for the scaled cooling of cryogenic fluid on the lunar surface is already being developed through NASA's Cryogenic Fluid In-situ Liquefaction for Landers (CryoFILL) program [8].

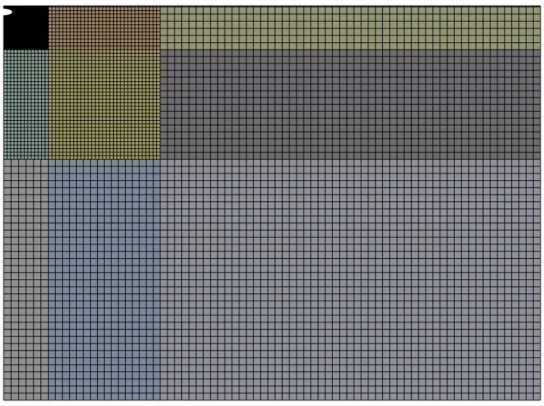

Figure 5: Simulation mesh, increasing with distance from METALS module (ellipse, top left) to optimize computational efficiency.

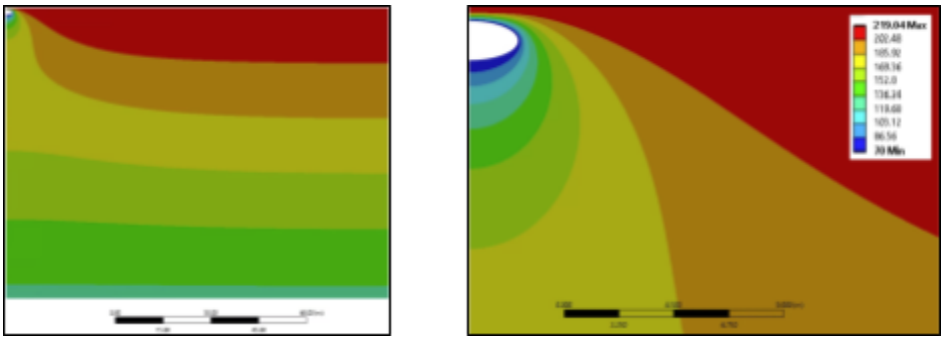

Figure 6: (a) Temperature plot (in Kelvin) around a buried METALS module (ellipse, top left). (b) Zoomed in view near the inflatable.

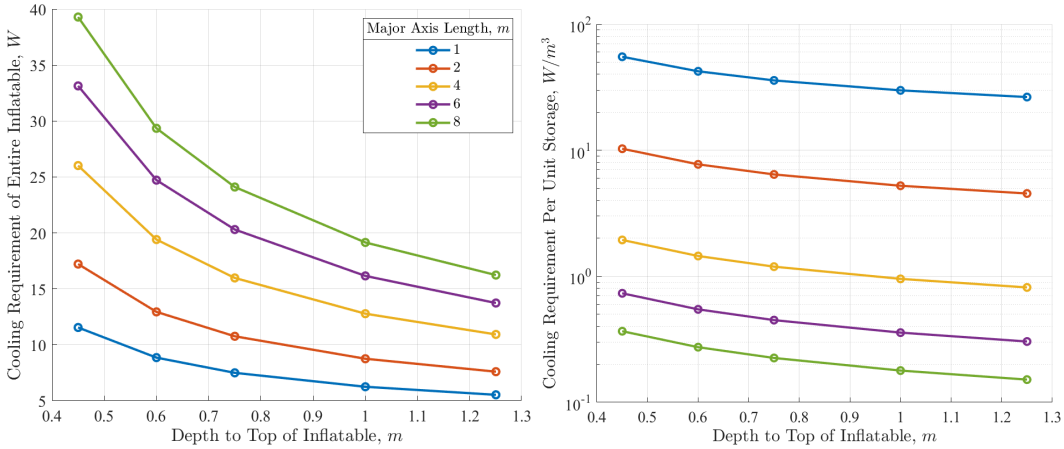

Figure 7: (a) Cooling power requirement (W) as a function of inflatable module depth (m) for different major axis lengths (1, 2, 4, 6, and 8 m). (b) Power requirement per unit volume (W/m^3) as a function of inflatable depth for the same major axis lengths. Results generated using finite element thermal analysis.

The above analysis investigates the cost associated with cooling an inflatable that is buried below regolith whose surface is exposed to direct sunlight. If mission planners desire to establish an Artemis basecamp in a region with consistent sunlight *and* keep fluid storage in close proximity to this station, then this is a realistic scenario. However, many other mission configurations can result in feasible cryogenic fluid storage, which are detailed in Section 5.1.6.

3.2.11 Selection of Burying Depth

Burying the metal inflatable may initially raise concerns of the ability of the inflatable to resist the weight of the regolith above it. However, the pressure pushing down on the inflatable will never approach the magnitudes of the stored fluid pushing outward (based on the target storage pressures described in Section 3.2.9). DSNE described a regolith density of approximately ~1600 kg/m^3 [5]. When combined with the Moon's low gravitational acceleration, the hydrostatic pressure exerted on the inflatable by the regolith will above it will increase at a rate of just $\rho g = (1600\ kg/m^3)(1.625\ m/s^2) = 2.6$ kPa/m, or 0.115 PSI/ft. In fact, the regolith above the inflatable will exert a force downwards against the pressure of the fluid inside the inflatable that pushes outwards. As a result, the presence of regolith above the inflatable will act to *reduce* the stress on the metal–a surprising effect that only improves with increasing burying depth. As a result, the compressive force on the inflatable by the regolith above it should not be considered in determining the ideal burying depth; instead, desired levels of micrometeorite protection, radiation shielding, and/or thermal insulation should be considered in comparison with the available excavation capabilities at the Artemis basecamp.

If an inflatable is somehow dented, buckled inwards, or crushed (caused by an accidental collision or other accident), then damage is easily repairable. One particular test series vertically compressed previously-inflated units using a hydraulic press. Not only did the inflatables support vertical loads/pressures of over 4537 lbf for 2mm thick stainless steel, many of the inflatables could be immediately repressurized and re-deployed to their prior inflated state. Other units experienced cracks within their welds that prevented them from being immediately inflated. However, welding repair techniques were also investigated and demonstrated (see Section 4.2.6 for details), illustrating that even an inflatable which loses the seal in its welds during compression could feasibility be repaired on the Moon and reinflated for future use, reducing the need to transport replacement units from Earth in the event of a damage incident or normal wear.

3.3 Testing Approach

At the conclusion of Phase I of the project, a reliable method for the manufacturing and inflation of METALS prototypes had been developed, as detailed in Section 3.2.6 above. In Phase II, several test campaigns were initiated to (1) study the scalability laws of the metal inflatable design through rapid manufacture and iteration, (2) evaluate the reliability of the proposed manufacturing methods through repeatable testing campaigns, and (3) evaluate the inflatable design within a variety of relevant lunar conditions to advance its flight-readiness to TRL 5 status.

Inflation pressure and shape testing assessed the reliability of the system across different pressures, shapes, and materials, helping predict how the inflatables would perform under various conditions. Standardized pressure testing created failure curves, demonstrating the inflatable's reliability under specific pressure conditions and establishing safety margins. Strength testing ensured the inflatables could withstand the weight of lunar regolith and other compressive forces, verifying their structural integrity. Cold environment testing demonstrated that the materials used in METALS could maintain their ductility in extreme cold, an essential feature for storing cryogenic fluids. Vacuum testing simulated lunar vacuum conditions to ensure the inflatables could hold pressure and function without atmospheric interference. Abrasion and micrometeorite resistance tests were conducted to confirm the durability of metals compared to polymers, especially under the harsh conditions of the lunar surface. Finally, heat transfer testing verified efficient thermal management for cryogenic storage, ensuring minimal heat transfer into

the vessel. Each of these tests was crucial in advancing METALS to the required technology readiness level, confirming that it meets the necessary standards for lunar infrastructure deployment.

3.4 Stakeholders

METALS technology directly interacts with several key systems: inflation sources, excavation tools, lunar pipeline integration, and electrical power for cryocoolers. Once installed, ongoing interactions are limited to the pipeline and cryocoolers, as stored fluids require transportation and cooling. This setup benefits developers of pipeline infrastructure and efficient cryocoolers, with short-term reliance on excavation and inflation technologies.

Artemis astronauts will benefit from METALS by having a reliable storage mechanism for large amounts of liquid oxygen. This enables them to focus on mission duties without concerns about oxygen supply and reduces energy expenditure associated with oxygen harvesting. Space organizations like SpaceX that need to refuel spacecraft en route from the Moon to Mars will also benefit. METALS's reliability and cost-effectiveness allow these organizations to transport cargo to Mars at lower fuel costs, enhancing the feasibility of long-duration missions. Equipment and infrastructure developers gain opportunities from METALS deployment. The demand for advanced pipeline systems and high-efficiency cryocoolers offers avenues for innovation and collaboration, while excavation and inflation technology providers are essential for initial deployment phases.

By engaging multiple stakeholders–from astronauts and space agencies to technology developers–METALS addresses immediate lunar mission needs and contributes to sustainable space exploration.

3.5 Risk Management

The following Risk Matrix identifies and evaluates potential risks to the METALS project beyond November 2024. Mitigation steps have been planned to address these risks.

1. Welding and material failures will be mitigated by using professional welders and robust testing protocols.
2. Safety hazards to astronauts during deployment are minimized by standardized inflation pressures, and can be completely mitigated by remote deployment.
3. Module designs can be simulated at larger diameters, ensuring large modules are best optimized.
4. Manufacturing reliability can be ensured through robotic welding and a standardized assembly process.
5. Irrepairability of modules can be proactively mitigated by incorporating a conservative safety factor into module operating inflation pressures.
6. Increasing material thickness will ensure that inflatables can handle operating pressures in the case that modules begin to fail as they are scaled.
7. Inconsistent deformation with pressure can be addressed by running experiments with controlling inflation nozzle size, different geometries, and speed of inflation.
8. Module designs can be simulated and tested to optimize for minimal buckling in the event of poor SEC scalability.
9. In the event of prolonged loss of cooling, critical failure of modules can be avoided by activation of a pressure release valve as cryogenic boil-off occurs, preserving the integrity of the inflatable.
10. Decreased ductility of the welds is expected even when using austenitic stainless steels. To mitigate this risk extensive failure probability analysis will be performed on inflatables expanded at RT and brought to failure at cryogenic temperatures. Additionally, post weld heat treatments to restore the austenitic phase may be a further derisking option.

METALS Risk Summary

ID	Summary	L	C	Trend	Approach	Risk Statement	Status	Criticality
1	Welding and Material Failures	2	5	↓	M	Given that the project relies on strong welding and material integrity, there is a possibility of failures during inflation, adversely impacting the structural integrity of the inflatables, which can result in catastrophic failure of the deployed structure.	Active	MED
2	Safety	1	5	↓	M	Given the nature of pressure vessels, there is a possibility of safety hazards during manufacturing, inflation, and testing, which can result in serious injury or damage to equipment.	Active	MED
3	Inflatable Scalability	2	3	→	R	Given that Artemis missions require the storage of large quantities of fluids, it is possible that the modules or systems of modules do not scale efficiently, adversely impacting large-scale storage capabilities.	Active	MED
4	Manufacturing Unreliability	1	4	↓	M	Given that the project relies on precise and durable welding, consistent manufacturing is a must. Ensuring consistent welds and processes is challenging and critical for the project's success.	Active	LOW
5	Irreparability of Modules in Vacuum of Space	1	4	↓	M	Given the harsh lunar conditions and extreme temperature/pressure gradients, it is possible that repairs to the inflatable will be difficult or impossible, adversely impacting module lifespan and operational continuity, which can result in mission-critical failures.	Active	LOW
6	Pressure Capabilities of Large Modules	2	3	→	R	Given the fact that pressure requirements for deformation decrease as module diameter increases, it is possible that pressure requirements for efficient fluid storage could exceed the capabilities of these modules, resulting in critical failure.	Active	MED
7	Consistent Deformation vs Pressure	3	2	↓	R	Given the multiple factors influencing module inflation, it is possible that the modules will inflate inconsistently, reducing their final volume and shape, which can compromise structural integrity and limit their operational functionality.	Active	MED
8	Buckling of Modules	3	3	↓	W	Given the potential for increased buckling in larger inflatables, there is a possibility that larger modules are more likely to experience structural failure, compromising their scalability and reducing the practicality of using large modules.	Active	MED
9	Cryogenic Resource Loss and Module Failure	2	4	→	R	Given that power outages and fluctuating temperatures can lead to unintended heat gain for cryogenic storage modules, it is possible that cryogenic boil off can occur, resulting in resource loss and pressure increases that could cause critical failure of module integrity.	Active	MED
10	Cryogenic Weld Embrittlement	3	3	→	M	Given that the modules will be exposed to cryogenic temperatures, there is a possibility of weld embrittlement, adversely impacting structural integrity and increasing the likelihood of module failure, potentially compromising long-term operational viability.	Active	MED

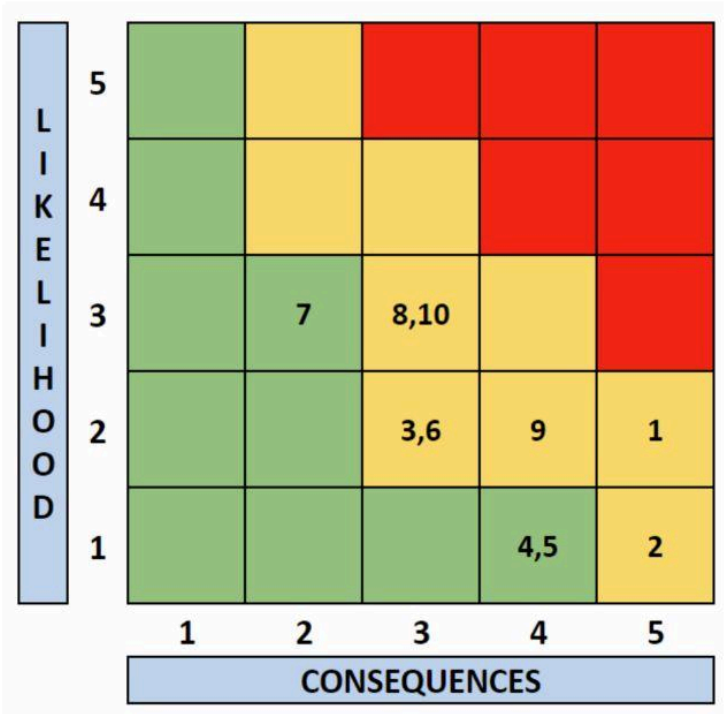

L = Likelyhood (1-5)
1 = not likely
5 = extremly likely
C = Consequence (1-5)
1 = low consequence
5 = high consequence

LxC Trend
↓ - Decreasing (improving)
↑ - increasing (worsening)
→ - unchanged
NEW - added this month

Approach
A - accept
M- mitigate
W - watch
R - research

Criticallity
HIGH
MED
LOW

4 Verification Testing on Earth

4.1 Overview

Verification for METALS was completed in eight thrusts: standardized inflation pressure, deformation as a function of pressure, inflation under vacuum conditions, cryogenic storage feasibility, micrometeorite impact resistance, reliability of welds, strength testing, and effect of annealing on carbon steel. Each experimental motivation, setup, results, and conclusion are outlined below. Together, these testing campaigns aim to demonstrate TRL 5 maturity for METALS technology.

4.2 Verification Tests

4.2.1 Standardized Inflation Pressure

Experimental Goals: This experiment aimed to validate the manufacturing reliability of metal inflatables, ensuring consistent performance across various geometries under controlled inflation conditions. A series of 15 inflatables were pressurized to failure across three distinct geometries: pentagon, hexagon, and optimized SEC. All inflatables were 12 inches in diameter and fabricated from 1 mm thick 304 stainless steel (Figure 8).

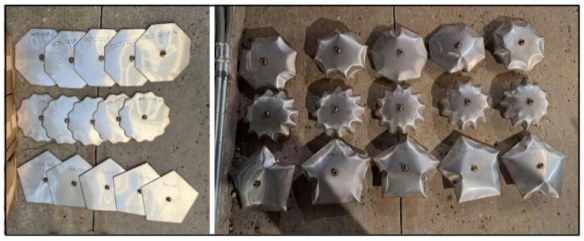

Figure 8: Modules pre and post inflation

Testing Procedure: Inflatables were submerged in water to measure displaced volume during inflation. Compressed air was introduced via a 4-way tee with a pressure gauge, release valve, and air hose. Displaced water exited into a bucket on a calibrated scale to measure air volume. Cameras recorded pressure and scale readings, while a Python script captured real-time data. For inflatables exceeding the 150 psi air compressor limit, a 3000 psi pressure washer was used, and the internal water volume was directly weighed.

Results: As shown in Figure 9, the pentagon geometry displayed significant volume variation at similar pressure points, with failure occurring between 27-67 psi. The octagon geometry (Figure 9, middle chart) exhibited a similar trend but increased volume inconsistency past 10 psi, with failure pressures ranging from 20-48 psi. In general, almost all inflatable designs tested exhibited this behavior of continuous deformation until stress concentrations caused the inflatable to burst. In contrast, the Sinusoidal Edge Curve (SEC) design rapidly and consistently reached its final deployed state at ~50 psi, while the lack of stress concentrations at the SEC's continuously-bending edge allowed it to withstand a remarkable range of additional pressurization before bursting at approximately 448 psi (total range of burst pressures for the five 12" SECs was 356 to 521 psi).

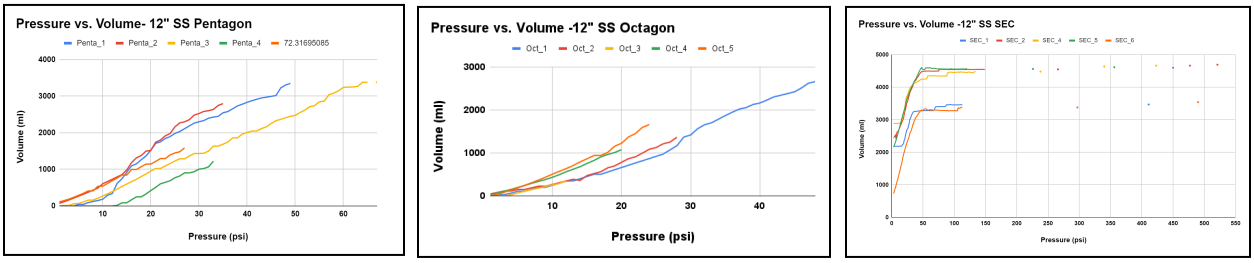

Figure 9: Volume vs. Pressure for 12" Stainless Steel pentagon, octagon and SEC geometries.

Key limitations include decreased accuracy of inflation through the water displacement method due to setup variations. A pressure source with higher capacity and finer control for gradual pressure increase can also be used. Improvements to the water displacement method could involve better calibration of

scales and volumetric containers. A more leveled, airtight setup would ensure controlled water flow, minimizing splashing and uneven filling.

Conclusion: Results indicate inconsistent behavior for octagon and pentagon geometries, while SEC samples exhibited superior consistency. All SEC inflatables withstood high pressures, displaying a deformation trend that plateaued around 50 psi, outperforming the pentagon and octagon in both failure pressure and volume.

4.2.2 Deformation vs. Pressure Testing

Experimental Goals: This testing aimed to analyze the relationship between module deformation and inflation pressure across key design variables—shape, material, size, and thickness—under lunar-like conditions. The results inform module reliability during deployment.

Testing Procedure: The procedure followed the previous section's instrumentation and safety protocols. A total of 24 samples, using two thicknesses (1mm, 2mm), two materials (Stainless Steel 304, Low-Carbon Steel 1008), and four geometries (SEC, pentagon, hexagon, octagon) were tested.

Thickness Results: 2mm-thick modules demonstrated greater resistance to deformation under pressure compared to 1mm modules, resulting in reduced hoop stress and enhancing structural integrity (Fig. 10). 1mm modules, with higher ductility, buckled more easily, leading to earlier failure between 25 and 50 psi, while 2mm modules resisted failure beyond 125 psi. Therefore, increased thickness raised the failure threshold by absorbing more stress before yielding but reduced flexibility, limiting expansion.

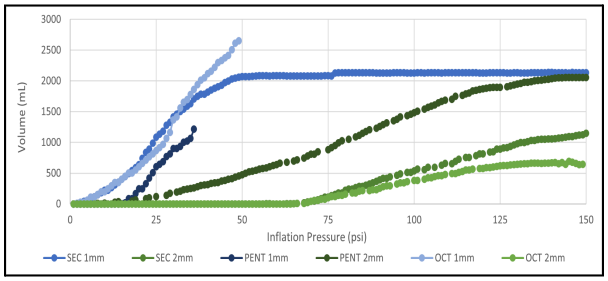

Figure 10: Effect of Thickness on Deformation vs. Pressure Testing for Stainless Steel 304, 12'' diameter modules. Blue-toned lines represent 1mm, while green-toned lines represent 2mm.

The SEC geometry uniquely resisted failure regardless of thickness, exhibiting initial deformation rates similar to other 1mm-thick geometries but resisting failure until pressures above 150 psi. The sinusoidal crests and troughs distributed stress effectively, preventing localized buckling and enabling higher pressure performance where other geometries failed.

Material Results: Material selection impacted burst pressure. While Low-Carbon Steel and Stainless Steel 304 produced similar final volumes, the burst pressure of Stainless Steel 304 reached up to 616 psi (Table 4), highlighting its superior longevity and pressure tolerance.

Table 4: Average Final Volume & Burst Pressure for 12'' diameter, SEC geometry modules.

	CRS SEC 1mm	CRS SEC 2mm	SS SEC 1mm	SS SEC 2mm
Burst Pressure (psi)	273	417	440	616
Final Volume (mL)	4538	5447	4425	5450

Geometry Results: The SEC geometry displayed the most uniform deformation and highest pressure resilience, resisting failure beyond 150 psi regardless of thickness. This design's sinusoidal crests and troughs effectively distributed stress, minimizing localized buckling. In contrast, polygonal geometries experienced stress concentrations at vertices, leading to earlier failure from buckling. Overall, analysis on the scalability of the solution in terms of varying diameters is recommended. Future experiments should utilize machine-based welding to achieve higher consistency in the results.

Conclusion: The deformation vs. pressure tests confirm that the proposed module geometry, the SEC, meets structural integrity and pressure resistance requirements for lunar deployment. These designs demonstrated scalability and durability, with potential for broader mission scenarios. Further testing could optimize performance across other dimensions and materials.

4.2.3 Vacuum Testing

Experimental Goals: Vacuum testing was conducted to assess the operational reliability of metallic inflatables in simulated lunar conditions, where the absence of air creates pressure differentials that might cause structural failures. Inflation inside a vacuum chamber was conducted to determine the technology's capability to deform and retain pressure under vacuum conditions without collapsing or rupturing.

Testing Procedure: Modules were placed inside the Across International VIM2000 furnace and connected to an Argon tank. Pressure was monitored by a transducer. Once chamber pressure was lowered to 0.005 Torr, the modules were pressurized using a regulator with ~5 psi sensitivity, and pressure was held constant, measuring any fluctuations. After the test, the chamber was repressurized. Three tests were conducted with varying geometries and pressures. The initial setup utilized Yor Lok connections, but due to a manufacturing error, the final two tests used NPT fittings sealed with Teflon tape.

Table 5: Vacuum testing summary

Geometry	Diameter (in)	Storage Pressure (gauge, psi)
SEC1	7.5 in	8.380844 psi
SEC2	6 in	39.15852 psi
Pentagon	6 in	49.35412

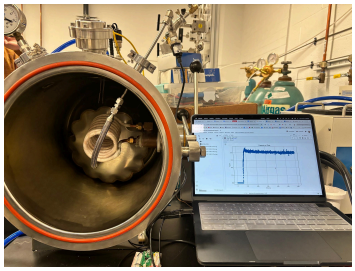

Figure 11: Vacuum Testing Setup.

Results: All three inflations were successful, with no bursts at pressures above 50 psi, and the inflatables held pressure with leak rates below 0.02 psi/s. The first test, with Yor Lok connections, presented the lowest leak rate of 0.0012 psi/s. Tests two and three, using Teflon tape seals, observed higher leak rates, 0.0073 psi/s and 0.0110 psi/s respectively, likely due to seal conditions. Final pressures represented 97.61%, 97.03%, and 96.85% of their initial values for tests 1, 2, and 3, respectively. However, manual pressure control via valve twisting caused inconsistent inflation and pressure spikes, as seen in the graphs. Misfitted modules increased leakage, and NPT connections on the pressure sensor contributed to the issue. Variations in shape, size, and pressure rates further hindered data consistency, complicating comparisons.

Conclusion: Test results confirm the design operates successfully in a vacuum. All three vacuum inflations were successful, with no bursts at pressures comparable to those at atmospheric pressure. While the inflatables held pressure after reaching the target value, external factors caused a high leak rate, as detailed in the Limitations section, unrelated to the inflatable's actual pressure-holding capability demonstrated in the Holding Pressure test.

4.2.4 Cryogenic Storage

Experimental Goals: Certain metal crystalline systems present decreasing fracture toughness of welds at cryogenic temperatures. Furthermore, welding can induce phase transformations which may make austenitic stainless steels perform worse at these temperatures (Ding et al.). As inflatables are anticipated to store liquid oxygen fuel, cryogenic testing is necessary to ensure they do not fail in such scenarios.

Testing Procedure: Two methods were developed to assess the effects of cryogenic inflation on design parameters. To ensure safety, inflations occurred in an impact-resistant polycarbonate cube, with

personnel wearing lab coats, safety glasses, and cryogenic gloves. Method 1 measured volumetric expansion and material characteristics. Two modules (SEC geometry, 7" diameter, 1mm thickness, Stainless Steel 304) were cooled to 171K and 103K, compared to a control at 280K, then pressurized to 85 psi. Temperature and pressure were recorded, module height was measured, and 3 cross-sections per inflatable were nano-indented to calculate yield strength. Method 2 tested failure points. Two modules were inflated to 85 psi at 280K, with one cooled to 171K. Both were pressurized to 150 psi, the maximum pressure reached by the air compressor.

Results: Table 6 demonstrates that inflation height and burst pressure decreased in relation to module temperature during inflation. Lower height increase and burst pressures were observed in initially cooled modules (Method 1), showcased by the lowest failure at 85 psi from the module at 101K. Meanwhile, the hardness values in Figure 12 suggest a post-inflation yield strength of roughly 300 MPa adjacent to the welds. There was no significant variation between the post-inflation hardness with inflation temperature. In the second experiment, the inflatable at 288K again had higher inflation; however, the 171K inflatable did not fail below or at 150 psi.

	Initial Temperature (K)	Inflation Height (in)
Method 1	103	0.763
	171	0.790
	288	1.691
Method 2	171	1.67
	288	2.06

Table 6: Initial Temperature and Inflation Height for Methods 1 & 2.

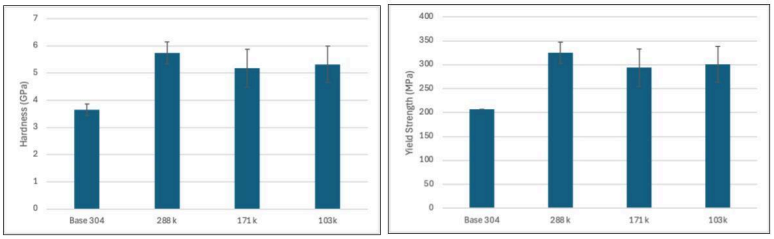

Figure 12: Nanoindentation results. Left: hardness values. Right: yield strengths extrapolated from the base SS 304 of 206.8 MPa (30 ksi).

Cryogenic inflation in vacuum faced safety concerns, as rapid boiling of liquid nitrogen could produce an explosion, disabling further testing to be conducted. Some modules were not inflated to failure due to the 150psi limit pressure of the air compressor, disabling the confirmation of METALS' improved strength when storing cryogenic fluids. The timeline limited the quantity of modules tested, disabling reliability from being assessed. Despite this, the promising results prove that these cryogenic inflatables are capable of holding high pressures.

Conclusion: As expected, modules inflated at room temperature showed greater height expansion, while those inflated at cryogenic temperatures had lower burst pressures due to the inverse correlation between yield strength and temperature. At room temperature, higher plasticity blunted stress concentrations at the air pocket-weld interface, preventing failure (see section 4.2.8.). Cryogenic samples lacked this blunting, causing weld failure. However, a cryogenic sample pre-inflated at room temperature withstood up to ~150 psi, indicating that pre-inflated METALS modules can maintain integrity for pressurized cryogenic storage. It is recommended to inflate METALS during the lunar day or after heating for optimal performance at cryogenic temperatures.

4.2.5 Micrometeorite Impact & Repairability of METALS

Experimental Goals: In the face of possible punctures from micrometeorites due to their high velocities, two repair solutions were developed for patching punctures on inflated modules. The purpose of this experiment was to evaluate the efficacy of the proposed solutions.

Testing Procedure: To simulate a puncture on the inflatable, a 0.223" hole was drilled into a 7'' diameter SEC and a 6" diameter octagon (both 1mm stainless steel 304). The solid-state solution involved clamping a 1x1 inch patch of the same material over the SEC puncture and TIG welding it with 45 amps. The liquid-state solution used MIG welding between 20 and 25 Amps, applying filler material in a converging spiral. The effectiveness of both methods was tested by applying soapy water to the welded

area, and introducing compressed air; the patch was deemed successful if no bubbles formed; indicating a leak-free seal.

Results: The 7-inch inflatable SEC and 6-inch inflatable octagon were successfully patch-welded, with no leaks detected at the patched areas in both cases. Air pressure was increased up to 55 psi without any visible issues for either inflatable. However, the solid-state solution struggled with welding lap joints due to inflatable curvature, requiring testing on partially inflated surfaces. The liquid-state solution became more complex with larger punctures, increasing the size of the hole instead of repairing it. Future tests should target inflatables with greater curvature, larger punctures, or punctures near edge-welded zones to better simulate real-world conditions and assess effectiveness.

Figure 13: Repaired Modules with solid-state (1, 2) and liquid-state (3, 4) solutions.

Conclusion: The solid-state solution proved to be most effective for larger punctures due to its ability to cover wider areas. While the liquid state solution demonstrated to be ideal for smaller punctures, where filler adhesion is easiest.

4.2.7 Reliability of Welds

Experimental Goals: The primary goal was to assess weld reliability using X-ray micro-computed tomography, focusing on internal defects like voids, inclusions, or cracks. 3D images allowed precise detection of imperfections. Proving reliability on Earth is essential to ensure similar techniques can withstand the Moon's extreme conditions, where repairs are limited.

Testing Procedure: Three weld samples were taken (Table 7) by cutting out a corner of the weld after inflation (Appendix D, Figures 28, 29, and 30).

Table 7: Properties of Weld Samples

	Sample 1 (DECA 12-CS1):	**Sample 2 (SEC 12-SS1):**	**Sample 3 (PENTA 12-SS1):**
Length (mm):	34.9	42.4	19.2
Diameter (mm):	20.5	15.2	15.6
Material:	Carbon Steel 1008	Stainless Steel 304	Stainless Steel 304
Source of Welding:	In house welding	IMS Engineered Products	IMS Engineered Products

Using the SkyScan 1276 microCT, all samples were scanned at 6 µm resolution through full 360° rotation. The Amira software from Thermo Fisher Scientific (formerly FEI) enabled defect isolation, dataset alignment, and 3D visualization. The following table shares the precise parameters the samples were scanned under:

Table 8: SkyScan 1276 Micro-Computed Tomography X-Ray Parameters

Voxel Size (µm)	**Voltage and Current (kV, µA)**	**Filters**	**Exposure (ms)**	**Averages per Projection**	**Pixel Binning**	**Scan Time (minutes)**
18.5	100, 200	Al+Cu	230	2	2x2	30

Results: A total of 5,991 slice images were taken, creating 3D renderings of the samples. Samples 2 and 3 were defect-free, while Sample 1 had a porosity defect at the weld joint due to trapped air (Figure 14). This defect was segmented, showing lower metal concentration in the joint, based on the size of the

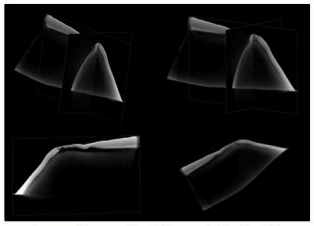

Figure 14: Double-Slice and Single-Slice Volume Renderings of Porosity Defect.

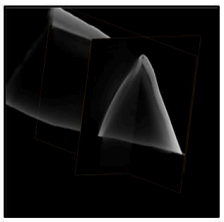

Figure 15: Double-Slice Volume Rendering of Largest Single Pore.

largest pore (Figure 15). It is important to note the variation in weld quality between samples due to variation in manufacturers' welding experience: Sample 1 was manufactured in-house by team members, while Samples 2 and 3 were professionally welded. However, larger samples reduced scan resolution, and only smaller cuts could be analyzed. Access to the microCT machine was delayed until late July due to a system bug.

Conclusion: Inflatable welds must be done by professionals. The major porosity defect in Sample 1 highlights the risks of inexperienced welding, such as breaches under pressure or void-induced stress. Ensuring high-quality welding is crucial for safety in extreme environments.

4.2.8 Strength Testing

Experimental Goals: While the regolith above a buried inflatable is not expected to produce loads that crush or buckle the module (see Section 3.2.11) significantly improved reliability and confidence in the mission scenario can be achieved if the inflatable can be reinflated after crushing, denting, or damage from any arbitrary damage scenario.

Testing Procedure: To determine the feasibility of reinflation, a series of inflatables were pressurized to their final deployed state, crushed flat using a Universal Testing Machine (UTM), and repressurized. SEC, hexagon, and octagon modules made of 1008 low-carbon steel or 304 stainless steel were all tested, with thicknesses of 1 or 2 mm and diameters ranging from 6 to 18 inches. Rubber disks (88.25 cm^2 and 380.13 cm^2) were placed on the top and bottom of each module for uniform load distribution.
After testing, some inflatables without failed welds were re-inflated using compressed air. The inflation height was measured and compared to the initial height, followed by a second compression test. This process was continued until weld failure, after which re-inflation was no longer possible.

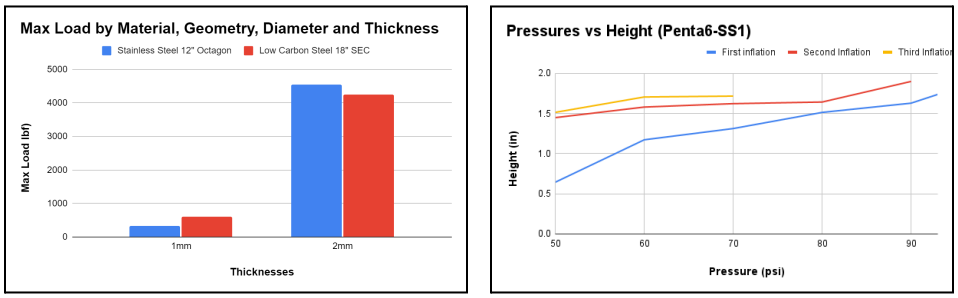

Figure 16: Max load of 12" Stainless Steel Octagons and 18" Low Carbon steel SEC with different thickness and re-inflation heights of Stainless steel 6" Pentagon

Results: Figure 16 (left) demonstrates that geometries with equal diameter and material, have significantly higher load capacities when designed with a thickness of 2mm. Additionally, Figure 16 (right) shows METALS' capability of re-inflation after compression. Modules were able to be inflated, compressed, and re-inflated two or three times, consistently presenting increased re-inflation heights for each relative pressure. However, load distribution uniformity was one concern; despite using rubber disks to prevent point loading, alignment or surface contact imperfections could affect results. Future improvements could involve using a larger UTM for bigger inflatables and testing at varied compression rates or dynamic conditions to better understand inflatable performance under different stress scenarios.

Conclusions: Some modules were able to match or exceed their initial height after re-inflation at the same pressure, suggesting a degree of resilience and potential for reuse. However, this can be due to material weakening from crack propagation and void expansion, as well as increased stress concentration at bend points, highlighting factors that affect long-term durability and performance under repeated use.

4.2.8 Effect of Annealing on Carbon Steel

Experimental Goals: The goal of this experiment was to see the benefits of annealing inflatables post welding. The anticipated results were (1) increased deformation due to softened matrix and (2) improved weld microstructure due to recrystallization.

Testing Procedure: A standardized specimen was made by welding two 10cm x 30 cm x 0.75mm AISI 1008 steel sheets (McMaster Carr, US) with a valve left for inflation. Both sample categories were cold rolled and formed into the spiral shape at room temperature. Half of the samples were annealed at 600 °C for 2 hours to measure the effect of annealing. The samples were cross-sectioned, mounted onto pucks and polished for imaging before being etched to show grain boundaries and measure grain size. Hardness testing was conducted with a nanoindenter (KLA iMicro) for pre and post-inflation mechanical values.

Results: Both the cold rolled and annealed inflatables were reliably inflated at 60 PSI and unrolled for linear actuation. The cold-rolled inflatable had a vertical displacement of 38.1 mm and the annealed inflatable had a vertical displacement of 42.9 mm. This demonstrates that annealing is an effective strategy for maximizing inner volume expansion. On the other hand, cold-rolled steel is still viable for linear actuation in cases where total volume expansion is not important such as with a truss.

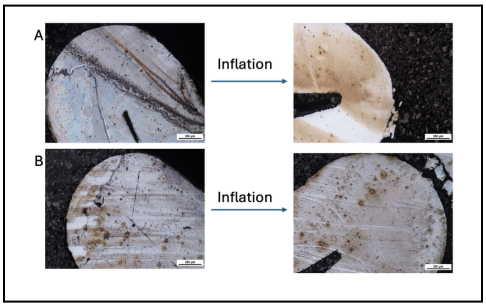

Figure 17: OM Images of low carbon steel pre and post inflation. A) Cold-rolled sample B) Annealed sample.

The OM images suggest that there was very high strain at the welds post inflation. Figure 17 shows the pre and post-inflation cross sections at the welds. The plate gap at the weld interface appears to at least double to the high degree of plasticity. Unfortunately, a quantitative measurement cannot be made due to the high variance in pre-inflation plate gap between replicates (1-20 microns). Fortunately, weld depth measurements show no correlation between pre and post-inflation weld depths, suggesting there is no fracture increasing the length of the plate gap. Therefore, it can be concluded that due to the high ductility of 1008 steel, the weld-gap interface self blunts decreasing the stress concentration and preventing fracture.

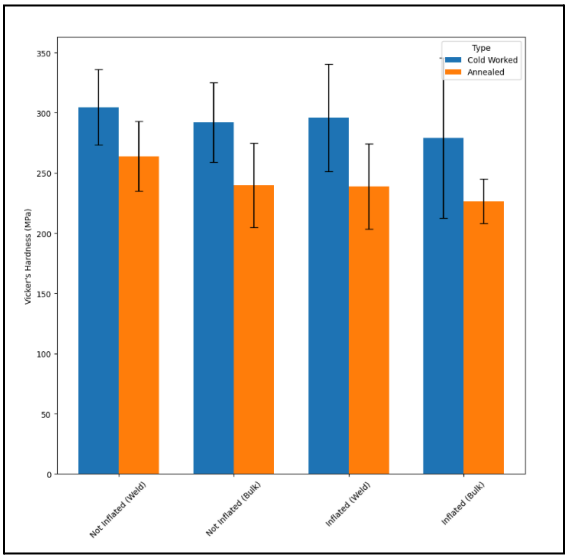

Figure 18: Pre and post inflation hardness for cold rolled and annealed mild steel samples

Pre versus post-inflation: The results from the Vickers hardness testing pre versus post- inflation are displayed in Figure 18. As expected, the annealed sample is softer in both the matrix and weld, as well as pre and post-inflated. This confirms that the annealing heat treatment was successful in softening the material and agrees with the results which showed greater deformation in the annealed sample. However, surprisingly the hardness is not significantly affected by the inflation itself. This means that the amount of cold working from the mild steel is not high enough to surpass the sensitivity of the instrument. While this is not beneficial for creating strong, work-hardened structures, it shows that the natural deformation of the material spreads out the stress evenly and prevents extremely high stress concentration at or near the welds. This spreading of stress was confirmed in an FEM model of the tested system.

5 Path-To-Flight

The METALS project has achieved significant technological readiness for its design requirements. However, to prepare for lunar operation, improvements to existing capabilities and exploration of additional systems are recommended. Several relevant future paths are detailed below.

5.1 Future Paths

5.1.1 Further Reliability Testing

A significant challenge which remains is how to verify the reliability of the METALS inflatable prior to launch. This will be accomplished with extensive statistical validation of the inflatables in vacuum. Additionally, a quality control process for verifying inflatable integrity should be implemented. Possible QC checks may include ultrasonic weld testing popular in the automotive and aerospace industries and a new method possibly using metal plates to prevent inflation while pressurizing the inflatables. Using ultrasonic weld testing, it is recommended that weld penetration is correlated to failure probability, and that this value is to set a standard which must be met in a given batch.

5.1.2 Scalability of Large Module Testing

METALS module sizes were limited by the external manufacturer, leading to minimal data in regards to more relevant large diameter modules and their respective failure pressures. Manufacturing scalability must be validated in order to efficiently produce larger modules. While preliminary data and engineering intuition suggests that thicker METALS modules will withstand higher pressure, further testing is required to optimize thickness and diameter for METALS to operate at the highest possible pressure, allowing for higher fluid storage temperatures and lower energy consumption of cooling systems. Additionally, as thickness increases, the need for higher weld penetration will increase, which may affect some of the process parameters. In order to control such parameters, robotic welding should be tested and analyzed for reliability as it can potentially offer better consistency than a welding professional. Lastly, different materials, specifically Ti64 and aluminum alloys, can be tested to potentially increase deployed volume-to-weight ratio and/or strength-to-weight ratio.

5.1.3 On-the-Moon Welding

In the event of micrometeorite impact or unexpected failure of METALS base material, modules can be repaired via patch welding. This process requires both a lunar welder and an operation plan in order to facilitate such repairs. Lunar Resource's PE3D welder has been proposed as a patch-welding solution for the Lunar South Pole Oxygen Pipeline [9], which could be applied to METALS given specific testing observing the case of welding the thin metal in vacuum. Once lunar welding capabilities are determined, testing would need to be completed to understand the extent to which metal systems can be manufactured and/or repaired on the surface.

5.1.4 Artemis Base Cryogenic System Integration

Cryogenic lunar infrastructure itself has yet to be fully developed, which presents many unknowns about the true capacity requirements of cryogenic storage and how it must integrate with other systems. Once this infrastructure is fully developed, METALS modules must be integrated and tested with compatible systems. A critical component is the development of a universal connection nozzle welded onto a module.

5.1.5 Excavation/Installation For Buried Modules

Regolith excavation for the installation of buried METALS modules remains to be a challenge requiring either excavation machinery or astronaut labor to achieve. NASA research suggests that excavation machinery will be available on Artemis base, centering the focus of METALS installation development on formulating an operation plan to emphasize astronaut safety and minimize both energy consumption and astronaut labor hours.

5.1.6 Optimize Thermal Management for Cryogenics

Further methods for feasible cryogenic storage have been identified to add flexibility of the METALS mission scenario, but must be simulated or experimented in order to quantify thermal benefits, energy consumption, and cost. In conjunction with burying under regolith, a light-weight "tarp" shade of low-emissivity material (such as aluminized Mylar, $\varepsilon \approx 0.044$) can be constructed above buried modules to block regolith absorption of solar flux, significantly reducing regolith temperatures by up to 60K [10], and thus the rate of heat transfer.

Within Permanently Shadowed Region (PSR) mean temperature of 18K, thermal management becomes an issue of heating, not cooling. This will be safely and reliably accomplished with resistive heating directly in contact with the module. Alternatively, liquid fuel can be pumped to the surface with reasonable efficiency since some energy is recovered on the way down. Additionally, fluid can be stored solid to increase storage density and reduce energy consumption, as heating is only necessary when fluid is to be transferred. This particular mission scenario may be especially energy efficient as continuous energy expenditure is not needed to maintain storage.

5.1.7 Thermal Management in Respect to NASA Organization of Artemis Base Resources

Thermal management must be adjusted to minimize cost and energy consumption based on the temperature requirements of the fluid stored, surface temperature of the environment, and whether or not the module is buried. Section 5.1.6 provides different methods of thermal management that can be applied to best suit the given scenario that NASA places a METALS module in.

5.1.8 Optimization of METALS Geometry for Efficient Packing

In order to reduce METALS footprint during transit, the geometry must be further considered. The current geometry of METALS is limited by the height of industry standard pipe fittings, at 12.7 mm tall. With custom fittings at half of the height, METALS would sit at only 8.35 mm tall. These custom fittings will require inflation tests to ensure their integrity throughout the forming process.

5.1.9 Heat Transfer Experimentation

Further improvements to heat transfer verification would be to conduct an improved experiment, which would consist of a buried-in-regolith METALS module filled with cryogenic fluid and connected to a cryocooler. This experiment would take place in a dusty thermal vacuum chamber at accurate regolith temperatures in order to emulate the lunar environment. With data collection from thermocouples, the temperature change would be recorded in the regolith and fluid in order to replicate the heat transfer of both Phase I and II. The results would be compared against simulation results, confirming the feasibility of buried METALS cryogenic storage.

6 Project Management

6.1 Project Leadership & Management

The 25 member team was managed by three team leads: Trevor Abbott, Julian Rocher, and Ben Taalman. For Phase I, the team was split into 3 sub-teams: manufacturing, analysis, and design, which were led by Abbott, Rocher, and Taalman, respectively. A full team meeting was held once every week for each sub-team to communicate progress, request assistance, and plan for the week ahead. A different member was required to present on behalf of his/her subteam each week in order to promote communication development and leadership among general team members. Each sub-team also held at least one meeting each week to divide tasks and brainstorm ideas. Outside of meetings, communication was done through a Slack channel throughout the project.

For Phase II, the team was reorganized with one 'lead engineer' and 2-3 team members for each type of verification testing. Additionally, Victoria Israel and Gavin Chung became team leads to help manage the increased complexity of the project. During the summer months, short meetings were held at 9am every morning for lead engineers to discuss their tasks for the day and any needs. Near the end of Phase II, the team moved to meetings twice a week in order to accommodate classes and increase work time.

Major decisions in Phase I were made using the OKR system by Abbott, Rocher, and Taalman with the help of Professors Ian McCue and Ryan Truby. While Phase I goals focused on demonstrating project viability and discovering the best application for the technology, Phase II goals focused on verifying the performance of METALS in relevant lunar environments and the reliability of manufacturing and inflation. In Phase II, all major decisions were made between team leads and lead engineers with the goals of each verification test in mind and a specific focus on proving cryogenic storage capabilities.

6.2 Project Schedule

The critical path for METALS is as follows: understanding the basic principles of metal inflation, including manufacturing methods and design parameters, choosing the optimal application for the technology, developing large scale reliable and consistent manufacturing methods, rapid prototyping and optimization of geometry, verifying scalable properties, and verification of technology in lunar environment. These items are what was expected for this project. Notably, the initial project proposal highlighted the importance of understanding the basic mechanisms of metal inflation and how it scales.

The detailed timeline below differs significantly from the initial proposal for two main reasons: 1) the use of hydrogen and oxygen combustion to inflate was completely scrapped due to safety and complexity concerns and 2) access to grant funding and ordering was severely delayed. The largest delay was processing manufacturing orders for IMS Engineered Products, which took on average a month to complete in addition to manufacturing time. To avoid major delays, team members were encouraged to learn how to weld and manufacture METALS modules using the Northwestern Segal Design Institute.

Phase I	March	• Team notified of finalist selection • Initial OKRs drafted. Team members are split into sub teams • Initial inflation simulations completed
	April	• First metal inflatable manufactured, inflated and analyzed • Preliminary METAL modules designed • Phase I funds processed by university • Began ordering equipment and materials • Discussions with IMS Engineered Products about manufacturing partnership
	May	• First professional inflatables are manufactured by IMS and inflated • Preliminary modular designs are manufactured and inflated • Heat transfer simulations begin • Team members begin welding training
	June	• End of Northwestern University spring 2024 finals week; start of summer work. • Research high priority use-cases for the METALS system, begin designing product prototypes. • Finalize service manufacturing contract with IMS engineering. • New set of modular designs sent to IMS for cutting and welding. • Complete fabrication and testing of safety set-up.
Phase II	July	• First iteration of IMS product prototypes inflated, data collected, and analyzed • Compression and 3-point bending tests completed on modules. Data is analyzed and relayed for implementation into prototypes. • Materials and components ordered for verification tests • Safety plan approved by Office of Research Safety • Storage vessels, specifically for cryogenics, is chosen as the most suitable application • SEC shape is designed and mathematically expressed. First prototypes are manufactured and inflated • Team members finish welding training • IMS order 2 is submitted for processing
	August	• SEC shape is optimized for maximum volume • 100s of inflatables are manufactured, tested, and analyzed
	September	• Submission of Fall Status Report. • IMS order received • Repeated testing of final inflatables to demonstrate reliability and consistency • Verification testing begins, including vacuum, strength, micrometeorite impact
	October	• Verification testing completed, including cryogenic, holding pressure, and heat transfer simulations • Submission of Technical Paper & Verification Testing Demonstration files.

6.3 Budget

6.3.1 Financial Overview

Overview Category	Budget (Phase I)	Budget (Phase II)	Actual Expenses (Phase I)	Actual Expenses (Phase II)	Balance
Total Direct Cost & F&A	$73,206.75	$73,214.10	$26,275.20	$88,764.85	$31,380.80
Direct Cost Total	$51,439.22	$40,774.44	$4,507.67	$56,325.19	$31,380.80

Breakdown by Expense Category

Expense Category	Budget (Phase I)	Budget (Phase II)	Actual Expenses (Phase I)	Actual Expenses (Phase II)	Balance
Non-Academic Temp, Work Study	$9,600.00	$14,400.00	$0.00	$11,065.00	$12,935.00
Supplies	$25,062.22	$2,200	$4,507.67	$20,175.21	$2,579.34
Services	$1,617.00	$6,544	$0	$25,084.98	-$16,923.98
Capital Equipment	$15,160.00	$0.00	$0	0.00	$15,160.00
F&A	$21,767.53	$32,439.66	$21,767.53	$32,439.66	$0.00

To date, METALS team spending has totaled approximately $115,040.05, around 78.6% of projected funding. Significant future expenditure includes domestic travel costs, which is estimated to be $20,000.00 for 15 team members to attend the Big Idea Forum in Las Vegas. Significant deviations include 1) savings of $12,935.00 due to $22,000.00 in awarded Northwestern summer research stipends from the McCormick School of Engineering and Summer Research Undergraduate Program, 2) zero capital equipment expense and an increase in services expenses from outsourcing manufacturing to IMS Engineered Products, 3) a decrease in supplies because IMS included supply charges as part of the services charge, and 4) a shift of Phase I charges to Phase II. Purchasing was severely limited near the beginning of the project as a result of financial processing delays within Northwestern University. Consequently, spending was carried out frugally at the beginning of the project and ramped up near the end. The shift to outsource manufacturing ultimately decreased overall costs and increased manufacturing quality. Budget constraints were approached carefully with time and quality as the main constraints.

6.3.2 Sponsorships and In-Kind Contributions

- IMS Engineered Products- at cost professional manufacturing services, estimated $15,000 total discount.
- National Aerospace Corporation- professional engineering consulting services, estimated at $5,000.
- McCormick Award Grant- 4 student stipends, $4,500 each, $18,000 total
- Summer Undergraduate Research Grant- 1 student stipend, $4,000 total
- Segal Prototyping Institute- use of professional welding equipment, estimated at $15,000

Total External Funding Estimation: $57,000

7. Appendix

Appendix A: Heat Transfer Simulation Conditions

Table of Boundary Conditions and Properties

Oxygen Properties	
Storage Temperature	70 K
Regolith Properties	
Emissivity at the South Pole (85-90 degrees S)	0.95 (DSNE)
Absorptivity	1 (Conservative Estimate)
Thermal Conductivity	0-2 cm deep: $0.9 \times 10^{-3} - 1.5 \times 10^{-3}$ W/m-K (DSNE) 2-25 cm deep: $1.0 \times 10^{-2} - 1.5 \times 10^{-3}$ W/m-K (DSNE approximation due to missing values from 15-25) 25+ cm deep: $1.72 \times 10^{-2} - 2.95 \times 10^{-3}$ W/m-K (DSNE approximation due to missing values from 25-35 and 234-9000)
Bulk Density	1.58 ± 0.05: (0-30 cm deep) g cm-3 1.74 ± 0.05: (30-60 cm deep) (DSNE)
Lunar Environment	
Surface Heat Flux	124 W/m2 (cos85 of solar heat flux)
Constant Temperature @90m depth	(41+224)/2 = 132.5 K

Appendix B: Pressure vs Volume Data
Below are figures displaying the results from pressurization tests performed on inflatables.

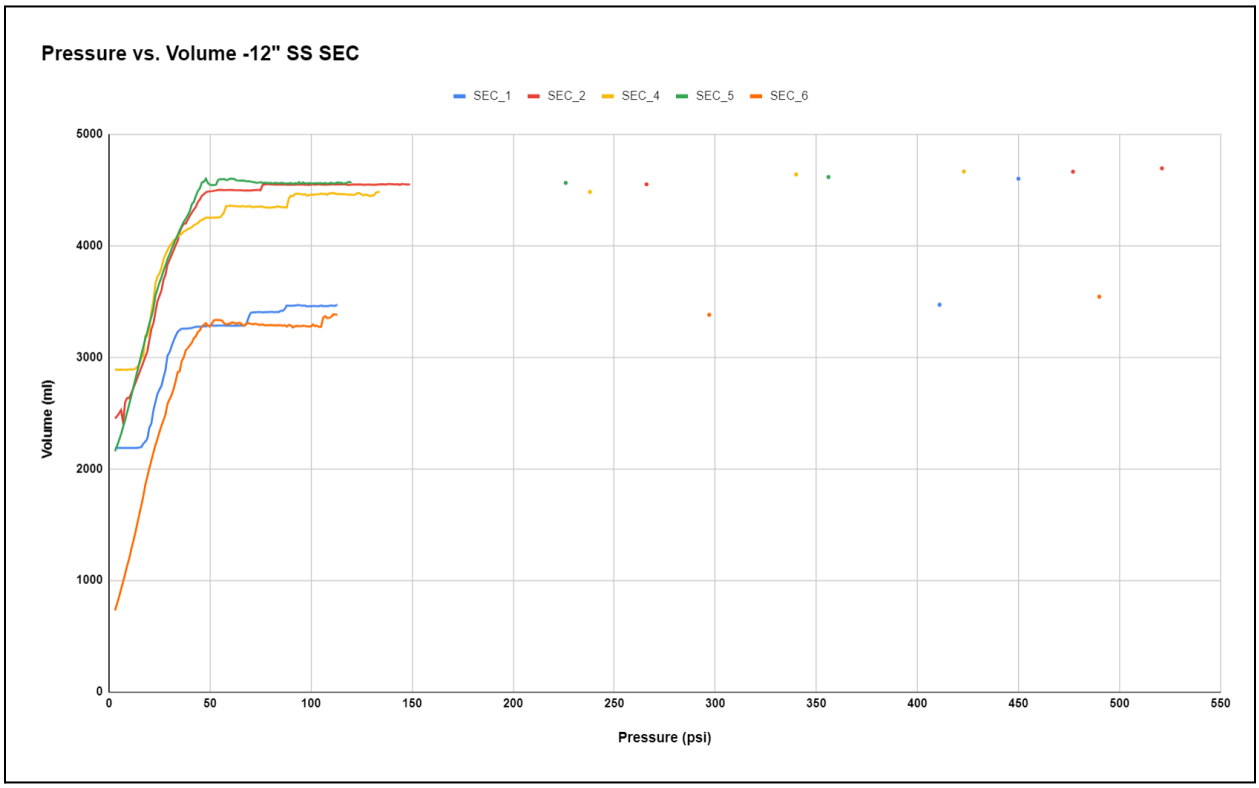

Figure 19: Pressure vs Volume for SEC Inflatables

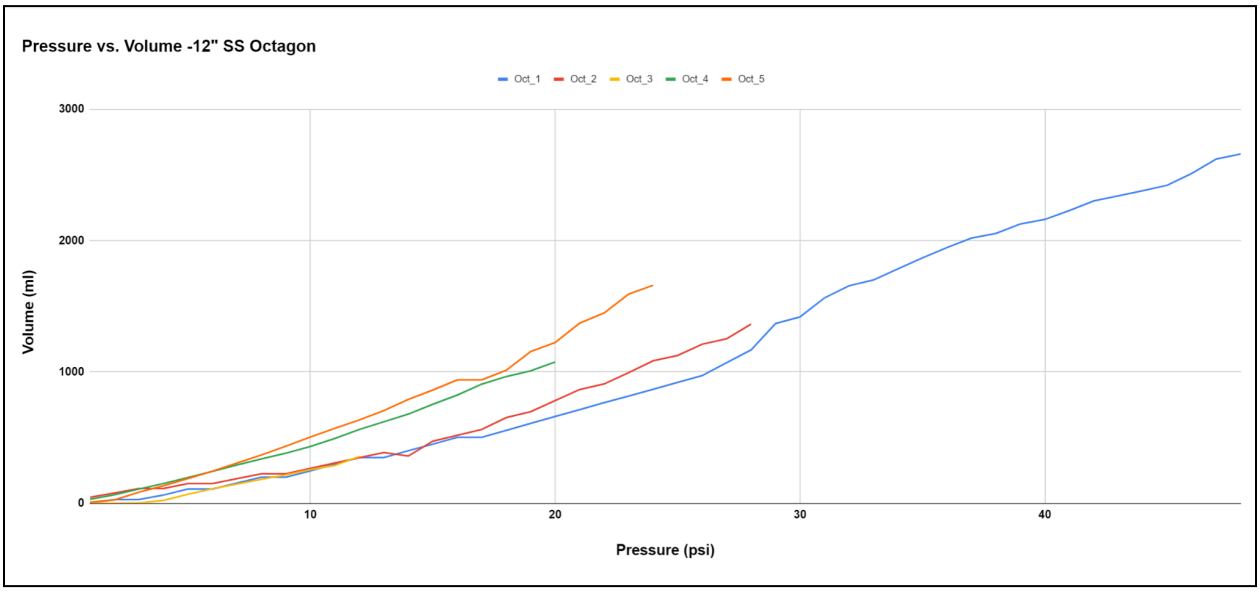

Figure 20: Pressure vs Volume Octagonal Inflatables

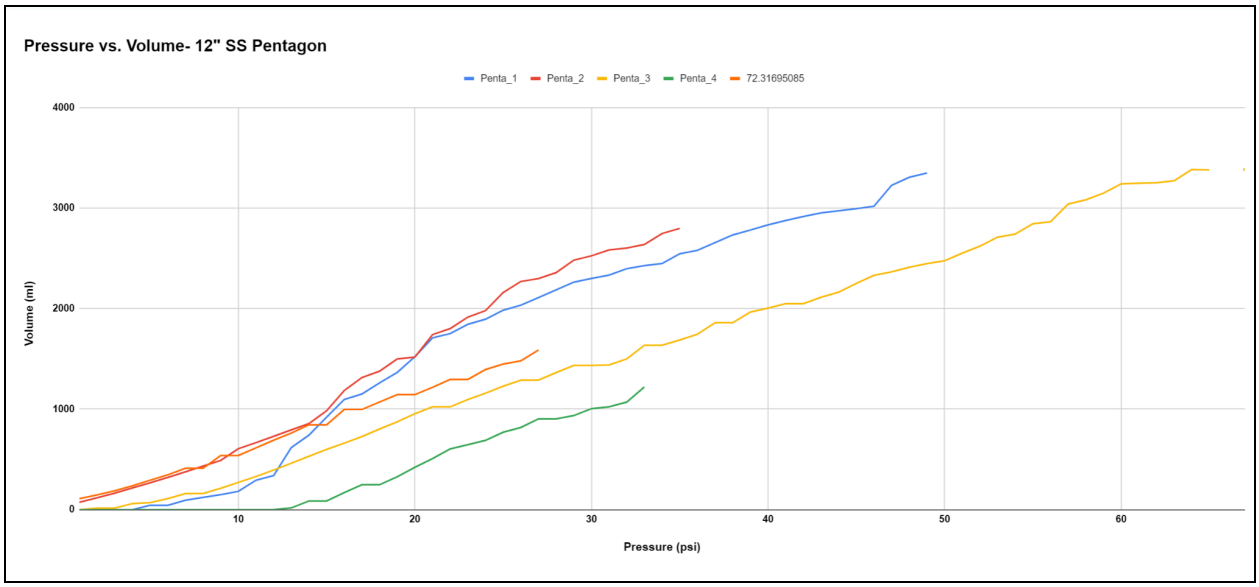

Figure 21: Pressure vs Volume Pentagonal Inflatables

Appendix C: Deformation vs. Pressure
Below are figures displaying how inflatable material thickness affected inflation.

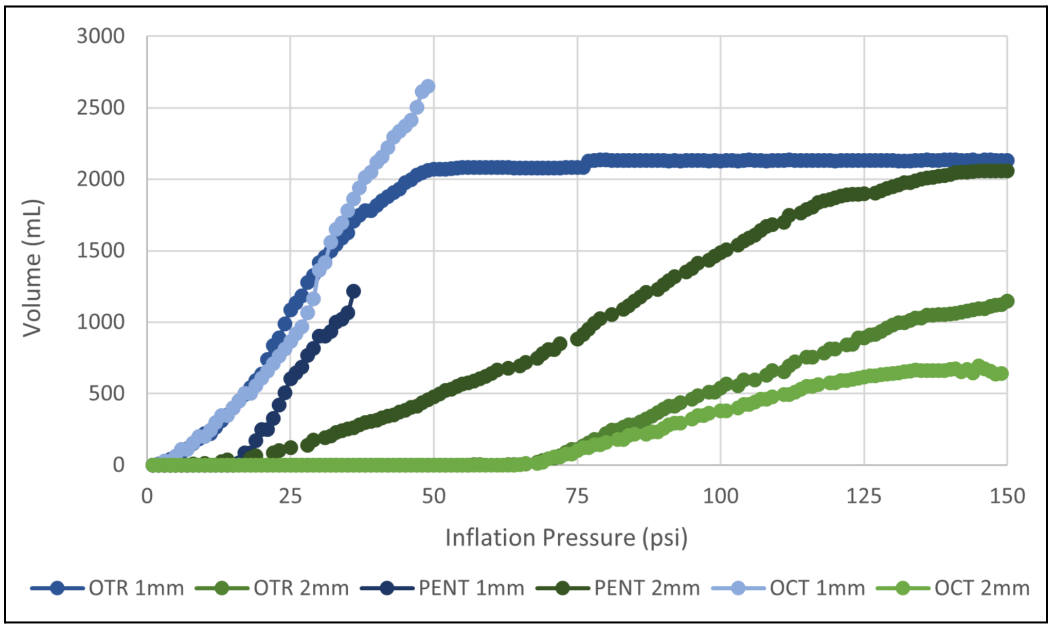

Figure 22: Performance of Inflatables by Thickness, Stainless Steel.

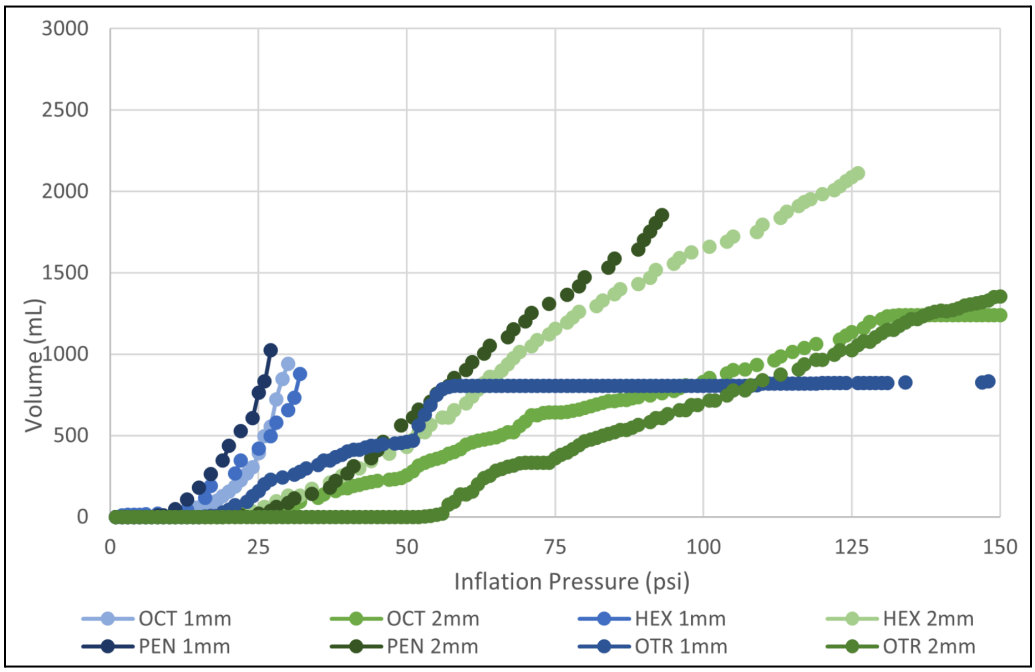

Figure 23: Performance of Inflatables by thickness, Low-Carbon Steel.

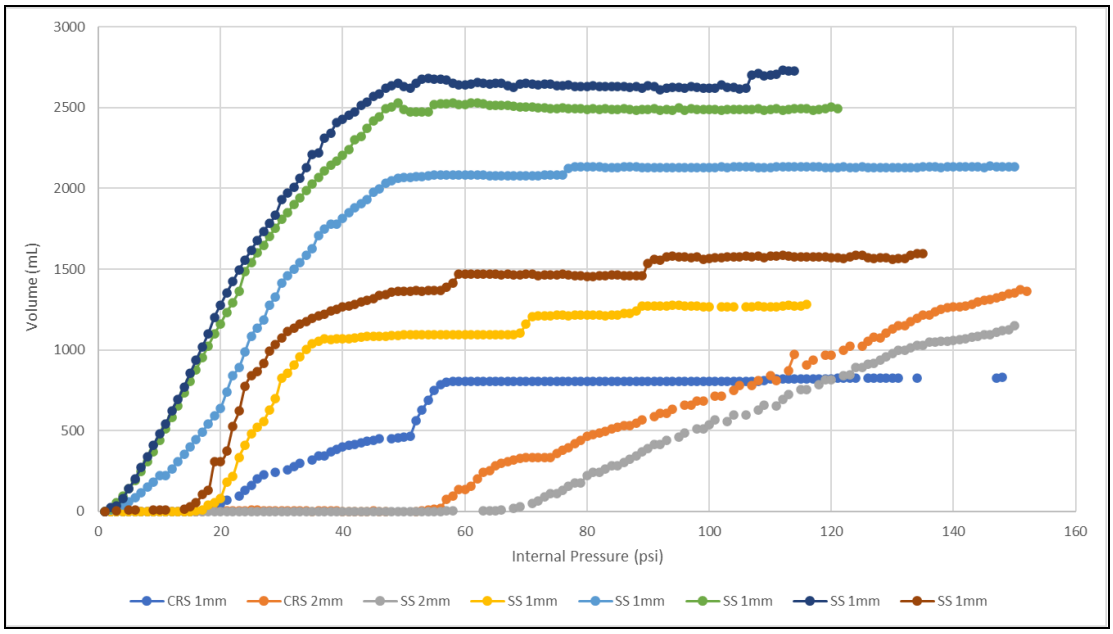

Figure 24: Performance of Inflatables by Material, SEC Geometry (all samples).

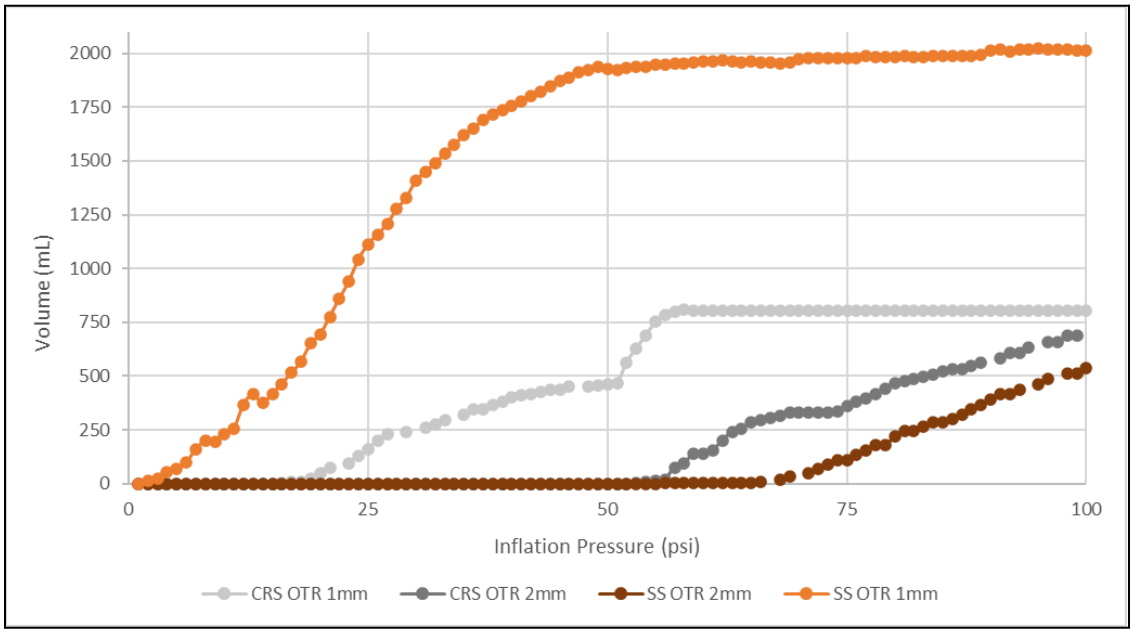

Figure 25: Performance of Inflatables by Material, SEC Geometry (summarized).

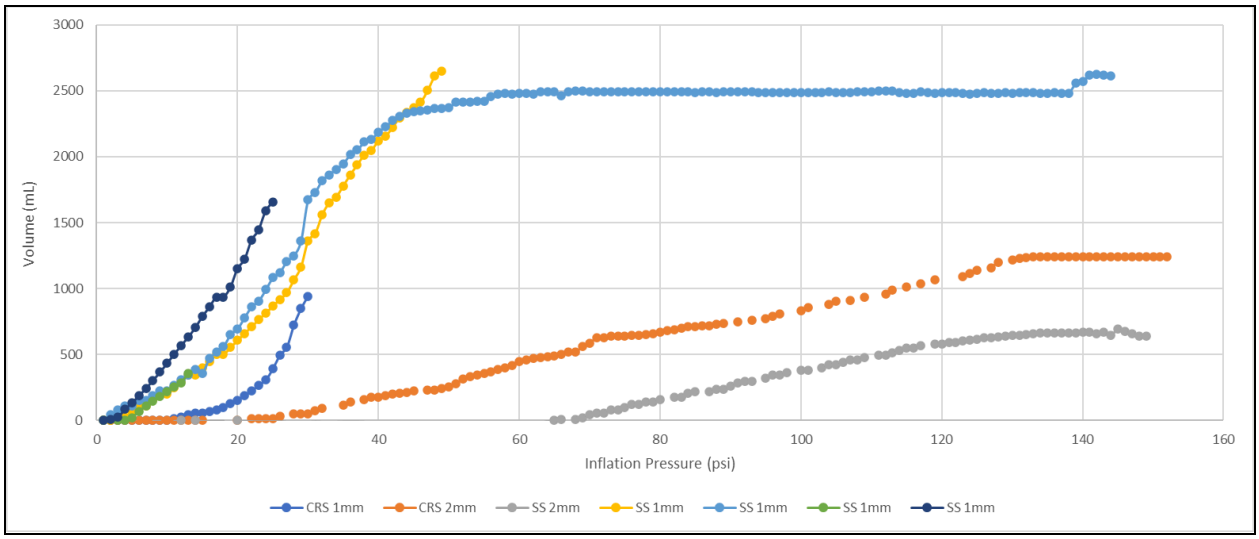

Figure 26: Performance of Inflatables by Material, OCT Geometry (all samples).

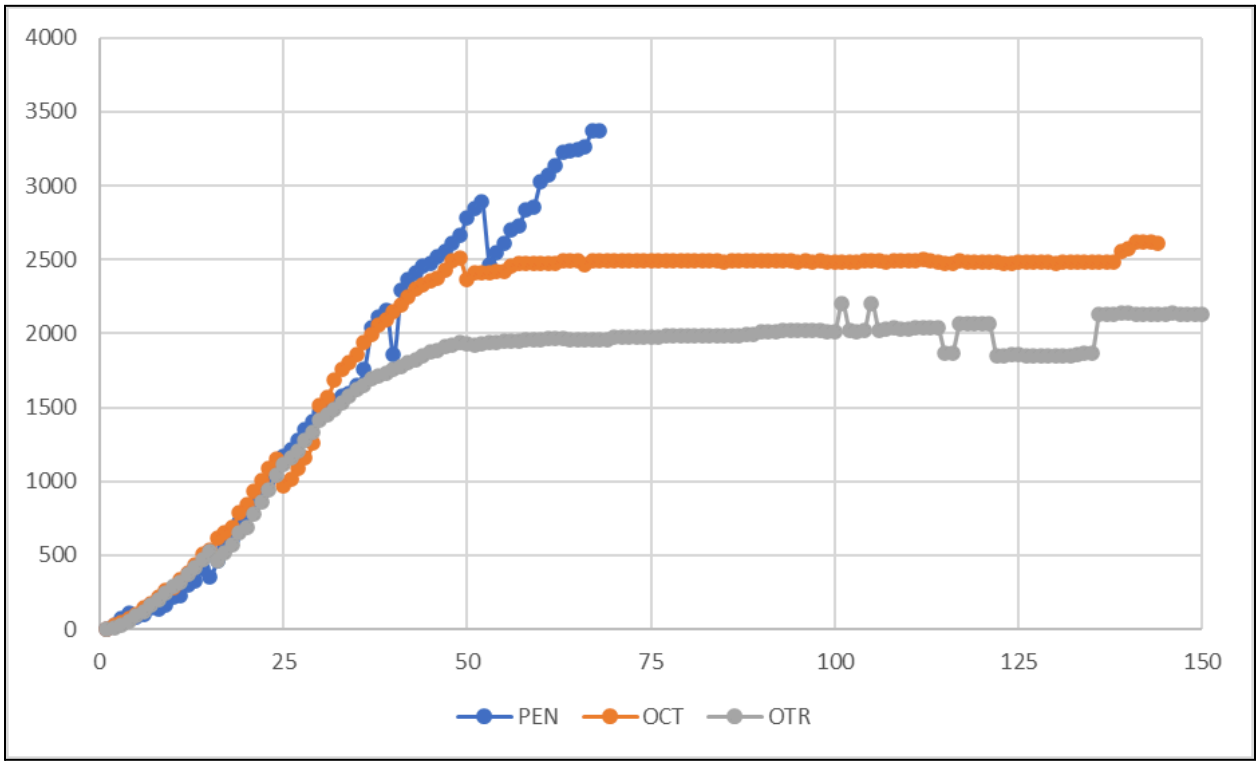

Figure 27: Performance of Inflatables Shape (PEN, OCT, SEC geometries).

Appendix D: X-ray Tomography Sample Images

Standard Sample Pictures:

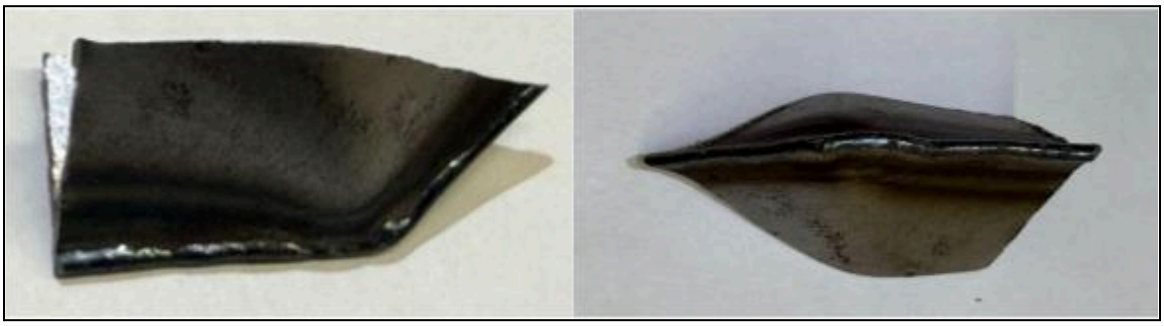

Figure 28: Sample #1 Reference Pictures (DECA 12CS1)

Figure 29: Sample #2 Reference Pictures (SEC 12-SS1)

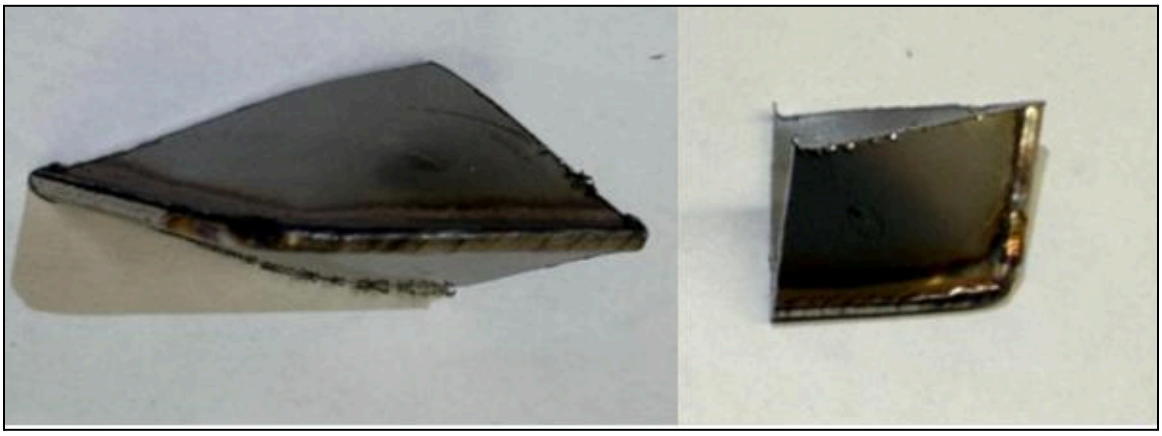

Figure 30: Sample #3 Reference Pictures (PENTA 12-SS1)

Sample X-ray Imaging Results:

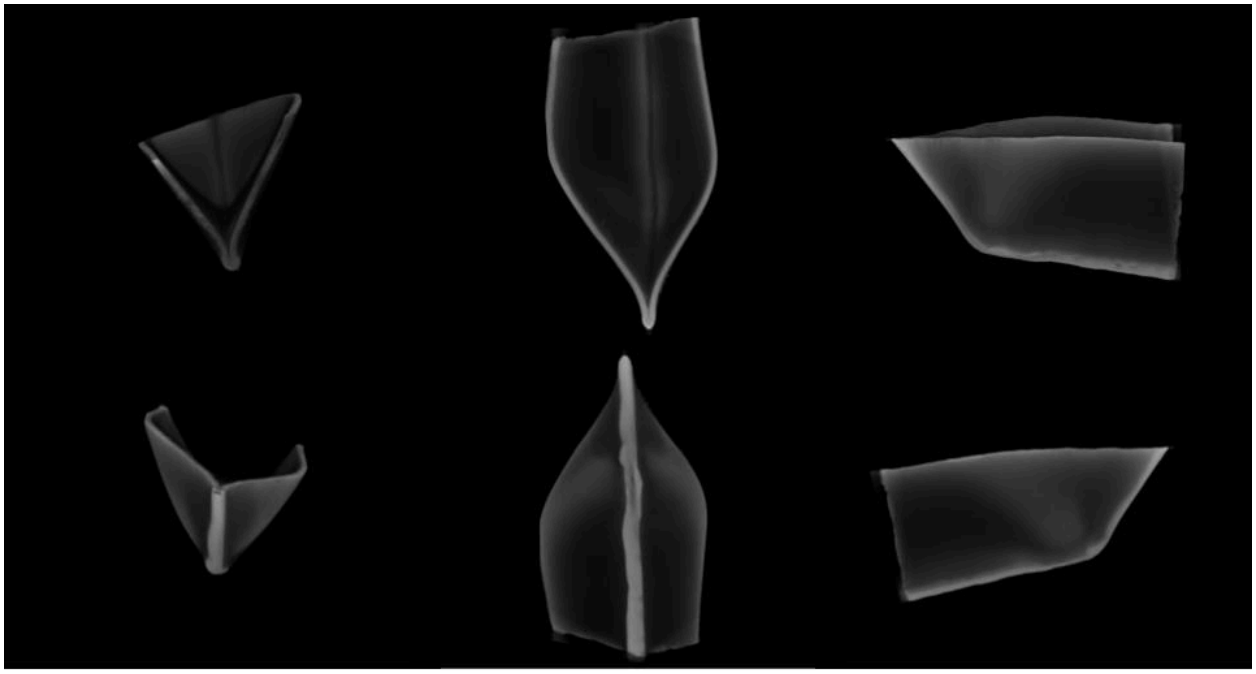

Figure 31: Axial Views of Standard Volume Rendering Views of Sample #1 (DECA 12CS1)

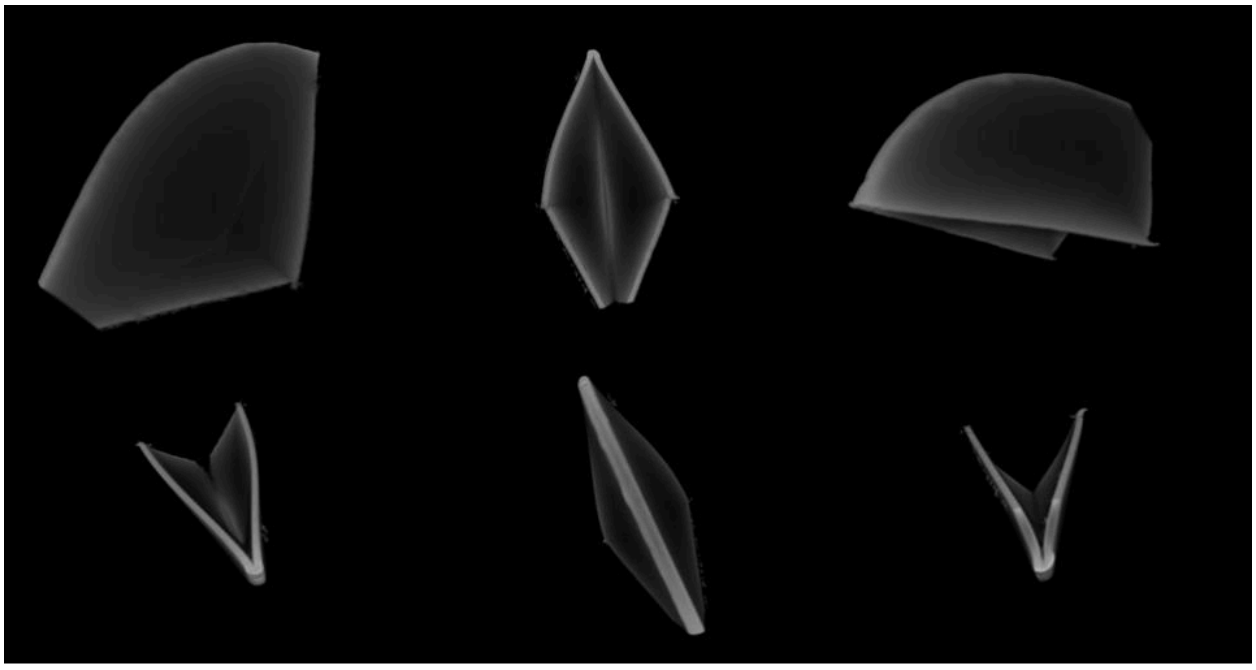

Figure 32: Axial Views of Standard Volume Rendering of Sample #2 (SEC 12-SS1)

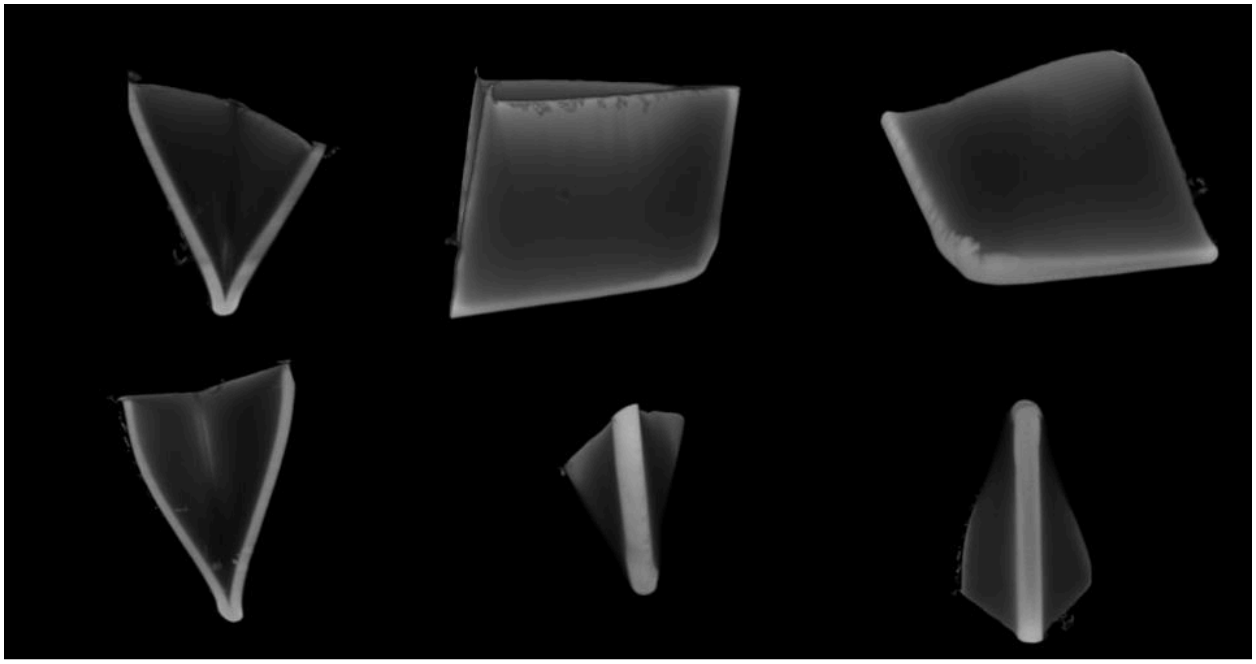

Figure 33: Axial Views of Standard Volume Rendering of Sample #3 (PENTA 12-SS1):

Appendix E: Vacuum Testing

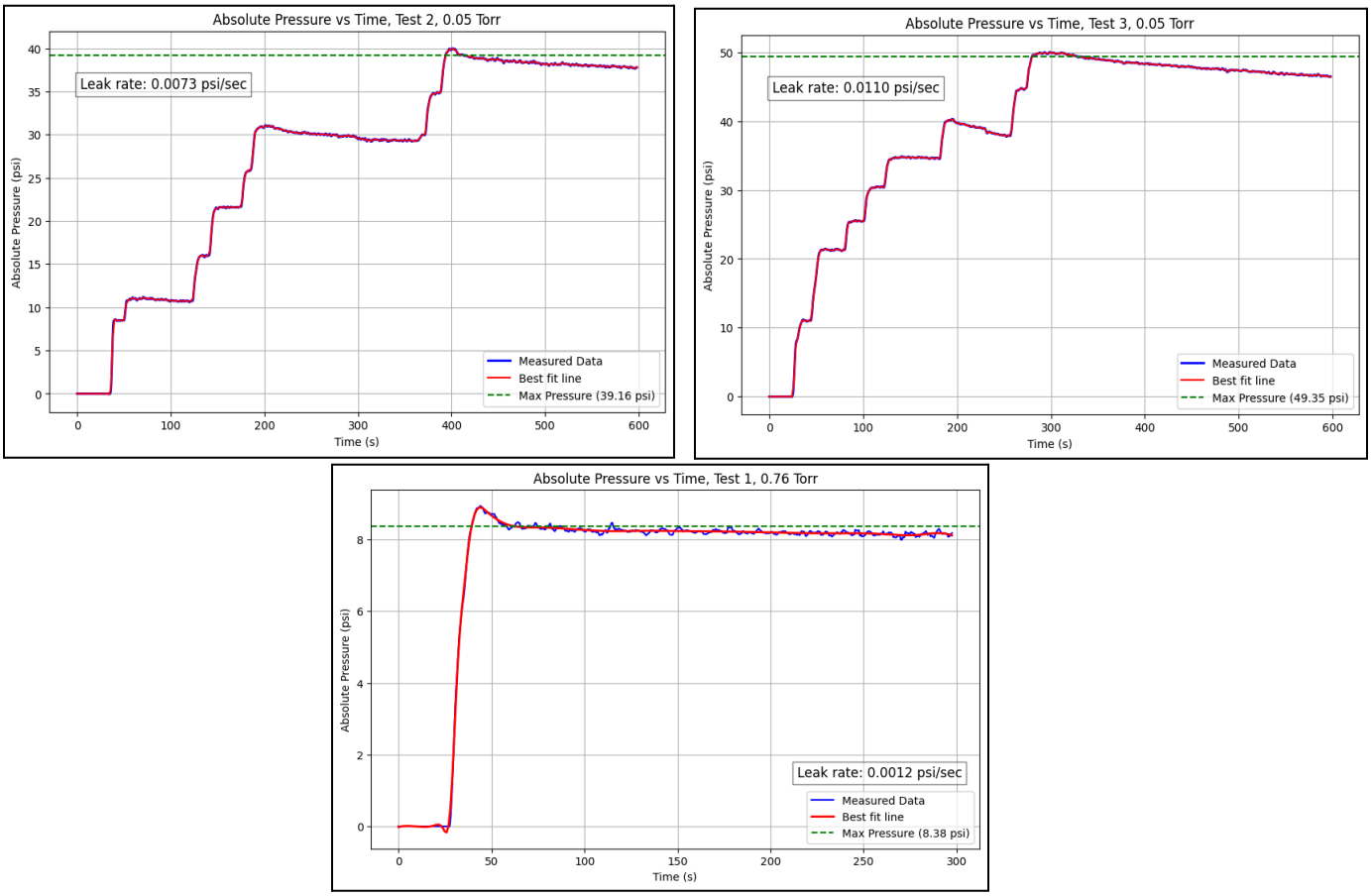

Figure 34: Inflatable pressure versus experiment time. Counterclockwise, beginning from the left, Test 1, Test 2, and Test 3.

Appendix F: Consistency in Inflation for SEC Inflatables

Final profile of deployed SECs were remarkably consistent, showing self-similarity across a range of diameters and sheet metal materials. These tests are included in the below figure.

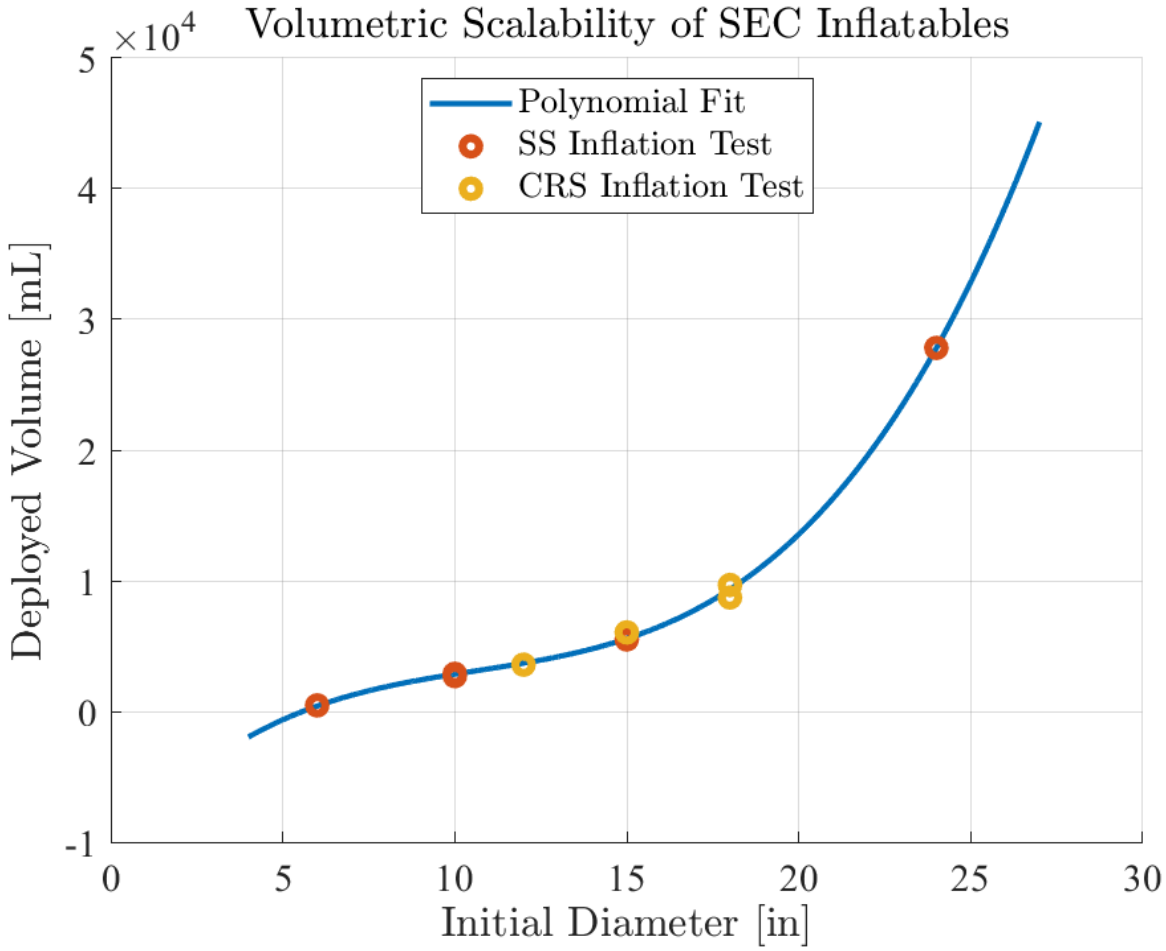

Figure 35: Inflatable deployed volume versus initial diameter for SEC inflatables of different materials.

Appendix G: Holding Pressure Testing

Experimental Goals
Holding pressure testing was conducted with the objective to evaluate the inflatables ability to maintain pressure over time.

Testing Procedure
Two geometries, OTR and Pentagon, both 12 inches in size and constructed from stainless steel, were inflated to 30 psi and observed for two weeks.

Results
The OTR module experienced a pressure loss on day 7 due to leaks in the Teflon tape at the weld, while the Pentagon maintained 30 psi at the two-week mark. This test demonstrated that with proper end caps at the buttweld, the modules are capable of holding pressure for extended periods on Earth.

Figure 36: Holding pressure setup.

Appendix H: Citations

[1] S. Mustafi, E. R. Canavan, R. F. Boyle, J. S. Panek, S. M. Riall, and F. K. Miller, "Active Co-storage of cryogenic propellants for lunar exploration," *NASA NTRS 20080039164*, 2008.

[2] B. C. Buckles, J. M. Schuler, A. J. Nick, J. D. Smith, and T. J. Muller, "ISRU Pilot Excavator - development of autonomous excavation algorithms," in *Space Resources Roundtable, XXII Meeting*, 2022.

[3] R. B. Malla and K. M. Brown, "Determination of temperature variation on lunar surface and subsurface for habitat analysis and design," *Acta Astronaut.*, vol. 107, pp. 196–207, 2015.

[4] G. Sanders and J. Kleinhenz, "In Situ Resource Utilization (ISRU) Envisioned Future Priorities," *Nasa.gov*. [Online]. Available: https://www.nasa.gov/wp-content/uploads/2023/06/live-isru-efp-new-3-21-23-tagged-1.pdf.

[5] S. Mustafi, E. Canavan, R. Boyle, J. Panek, and S. Riall, "Active Co-Storage of Cryogenic Propellants for Lunar Explortation," Nasa.gov. [Online]. Available: https://ntrs.nasa.gov/api/citations/20210024522/downloads/SLS-SPEC-159%20Cross-Program%20Design%20Specification%20for%20Natural%20Environments%20(DSNE)%20REVISION%20I.pdf. [Accessed: 17-Oct-2024].

[6] R. Lawler, "SpaceX's plan for in-orbit Starship refueling: a second Starship," *Engadget*, 29-Sep-2019. [Online]. Available: https://www.engadget.com/2019-09-28-starship-refueling-spacex.html.

[7] B. Ridgeway, "Fission Surface Power," *NASA*, 09-May-2023. [Online]. Available: https://www.nasa.gov/tdm/fission-surface-power/.

[8] *Nasa.gov*. [Online]. Available: https://ntrs.nasa.gov/api/citations/20230009751/downloads/LTF_CryoFILL_Overview_SCWPres_Johnson.pdf.

[9] L. Hall, "Lunar south pole oxygen pipeline," *NASA*, 09-Jan-2023. .

[10] X. Xiao, S. Yu, J. Huang, H. Zhang, Y. Zhang, and L. Xiao, "Thermophysical properties of the regolith on the lunar far side revealed by the *in situ* temperature probing of the Chang'E-4 mission," *Natl. Sci. Rev.*, vol. 9, no. 11, p. nwac175, 2022.